

Efficient Methods of Chaos Detection: Theory and Applications

Haris Skokos

**Max Planck Institute for Complex Systems
Dresden, Germany**

E-mail: hskokos@pks.mpg.de

URL: <http://www.pks.mpg.de/~hskokos/>

Outline

- **Hamiltonian systems – Symplectic maps**
 - ✓ Variational equations
 - ✓ Lyapunov exponents
- **Smaller ALignment Index – SALI**
 - ✓ Definition
 - ✓ Behavior for chaotic and regular motion
 - ✓ Applications
- **Generalized ALignment Index – GALI**
 - ✓ Definition - Relation to SALI
 - ✓ Behavior for chaotic and regular motion
 - ✓ Applications
 - ✓ Global dynamics
 - ✓ Motion on low-dimensional tori
- **Conclusions - Outlook**

Autonomous Hamiltonian systems

Consider an **N degree of freedom** autonomous Hamiltonian system having a Hamiltonian function of the form:

$$H(\overbrace{q_1, q_2, \dots, q_N}^{\text{positions}}, \overbrace{p_1, p_2, \dots, p_N}^{\text{momenta}})$$

The time evolution of an orbit (trajectory) with initial condition

$$P(0) = (q_1(0), q_2(0), \dots, q_N(0), p_1(0), p_2(0), \dots, p_N(0))$$

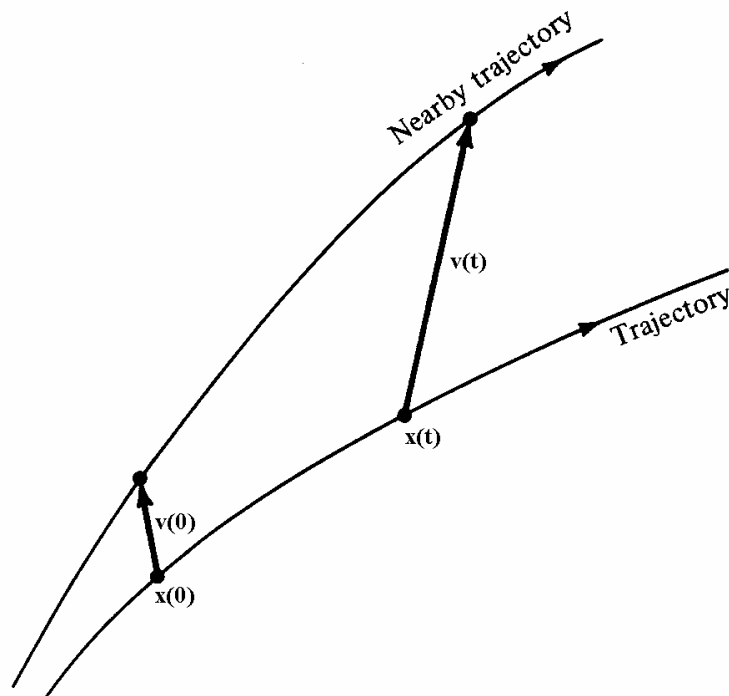
is governed by the **Hamilton's equations of motion**

$$\frac{dp_i}{dt} = -\frac{\partial H}{\partial q_i}, \quad \frac{dq_i}{dt} = \frac{\partial H}{\partial p_i}$$

Variational Equations

We use the notation $\mathbf{x} = (q_1, q_2, \dots, q_N, p_1, p_2, \dots, p_N)^T$. The **deviation vector** from a given orbit is denoted by

$$\mathbf{v} = (dx_1, dx_2, \dots, dx_n)^T, \text{ with } n=2N$$



The time evolution of \mathbf{v} is given by the so-called **variational equations**:

$$\frac{d\mathbf{v}}{dt} = -\mathbf{J} \cdot \mathbf{P} \cdot \mathbf{v}$$

where

$$\mathbf{J} = \begin{pmatrix} \mathbf{0}_N & -\mathbf{I}_N \\ \mathbf{I}_N & \mathbf{0}_N \end{pmatrix}, \quad P_{ij} = \frac{\partial^2 H}{\partial \mathbf{x}_i \partial \mathbf{x}_j} \quad i, j = 1, 2, \dots, n$$

Benettin & Galgani, 1979, in Laval and Gressillon (eds.), op cit, 93

Symplectic Maps

Consider an **2N-dimensional symplectic map T**. In this case we have **discrete time**.

The evolution of an **orbit** with initial condition

$$P(0) = (x_1(0), x_2(0), \dots, x_{2N}(0))$$

is governed by the **equations of map T**

$$P(i+1) = T P(i) \quad , \quad i=0,1,2,\dots$$

The evolution of an initial **deviation vector**

$$v(0) = (dx_1(0), dx_2(0), \dots, dx_{2N}(0))$$

is given by the corresponding **tangent map**

$$v(i+1) = \left. \frac{\partial T}{\partial P} \right|_i \cdot v(i) \quad , \quad i = 0,1,2,\dots$$

Lyapunov Exponents

Roughly speaking, the Lyapunov exponents of a given orbit characterize the **mean exponential rate of divergence** of trajectories surrounding it.

Consider an orbit in the $2N$ -dimensional phase space with **initial condition $\mathbf{x}(0)$** and an **initial deviation vector from it $\mathbf{v}(0)$** . Then the mean exponential rate of divergence is:

$$\sigma(\mathbf{x}(0), \mathbf{v}(0)) = \lim_{t \rightarrow \infty} \frac{1}{t} \ln \frac{\|\mathbf{v}(t)\|}{\|\mathbf{v}(0)\|}$$

Maximum Lyapunov Exponent

$\sigma_1=0 \rightarrow$ Regular motion
 $\sigma_1 \neq 0 \rightarrow$ Chaotic motion

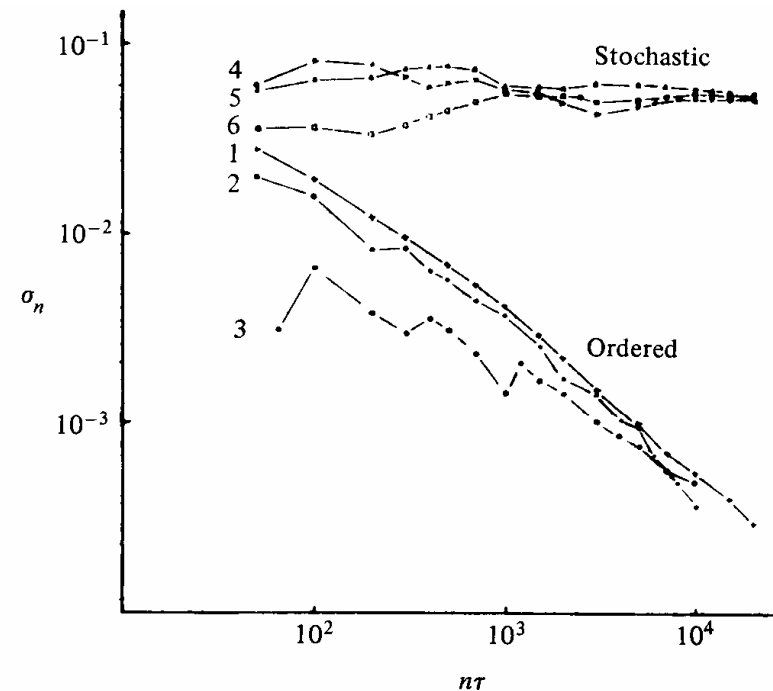


Figure 5.7. Behavior of σ_n at the intermediate energy $E = 0.125$ for initial points taken in the ordered (curves 1–3) or stochastic (curves 4–6) regions (after Benettin *et al.*, 1976).

If we start with more than one linearly independent deviation vectors they will **align to the direction defined by the largest Lyapunov exponent** for chaotic orbits.

Definition of Smaller Alignment Index (SALI)

Consider the **2N-dimensional** phase space of a conservative dynamical system (**symplectic map or Hamiltonian flow**).

An orbit in that space with initial condition :

$$P(0)=(x_1(0), x_2(0),\dots,x_{2N}(0))$$

and a **deviation vector**

$$v(0)=(dx_1(0), dx_2(0),\dots, dx_{2N}(0))$$

The evolution in time (in maps the time is discrete and is equal to the number n of the iterations) of a **deviation vector** is defined by:

- the **variational equations** (for Hamiltonian flows) and
- the equations of the **tangent map** (for mappings)

Definition of SALI

We follow the evolution in time of two different initial deviation vectors ($\mathbf{v}_1(0)$, $\mathbf{v}_2(0)$), and define SALI (**Ch.S. 2001, J. Phys. A**) as:

$$\text{SALI}(t) = \min \left\{ \left\| \hat{\mathbf{v}}_1(t) + \hat{\mathbf{v}}_2(t) \right\|, \left\| \hat{\mathbf{v}}_1(t) - \hat{\mathbf{v}}_2(t) \right\| \right\}$$

where

$$\hat{\mathbf{v}}_1(t) = \frac{\mathbf{v}_1(t)}{\left\| \mathbf{v}_1(t) \right\|}$$

When the two vectors become **collinear**

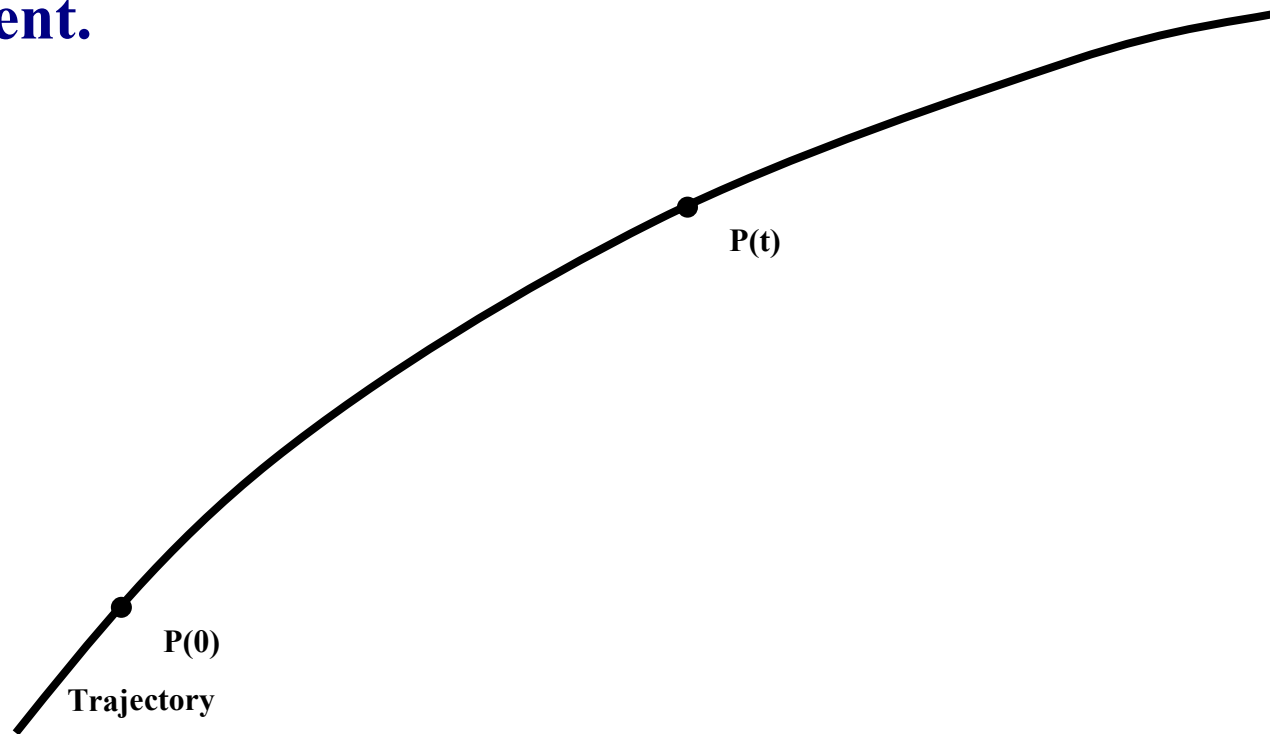
$$\text{SALI}(t) \rightarrow 0$$

Behavior of SALI for chaotic motion

For chaotic orbits the two initially different deviation vectors tend to coincide with the direction defined by the maximum Lyapunov exponent.

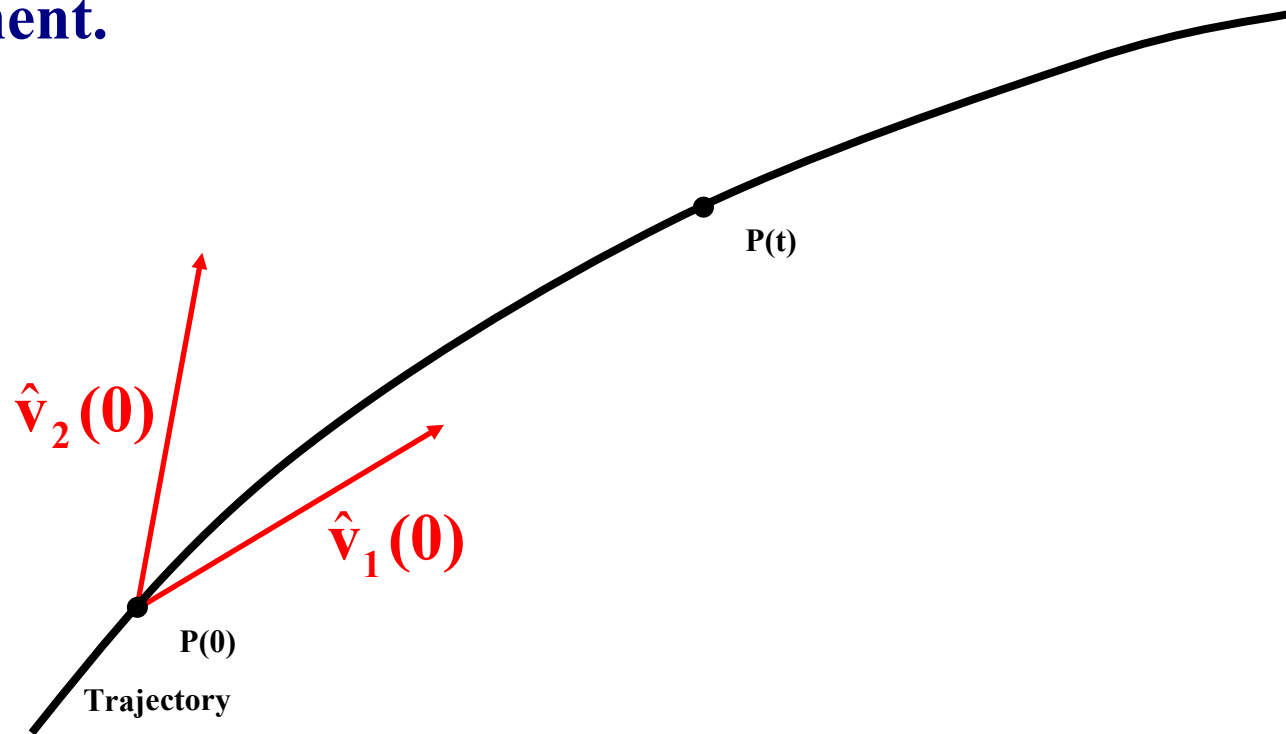
Behavior of SALI for chaotic motion

For chaotic orbits the two initially different deviation vectors tend to coincide with the direction defined by the maximum Lyapunov exponent.



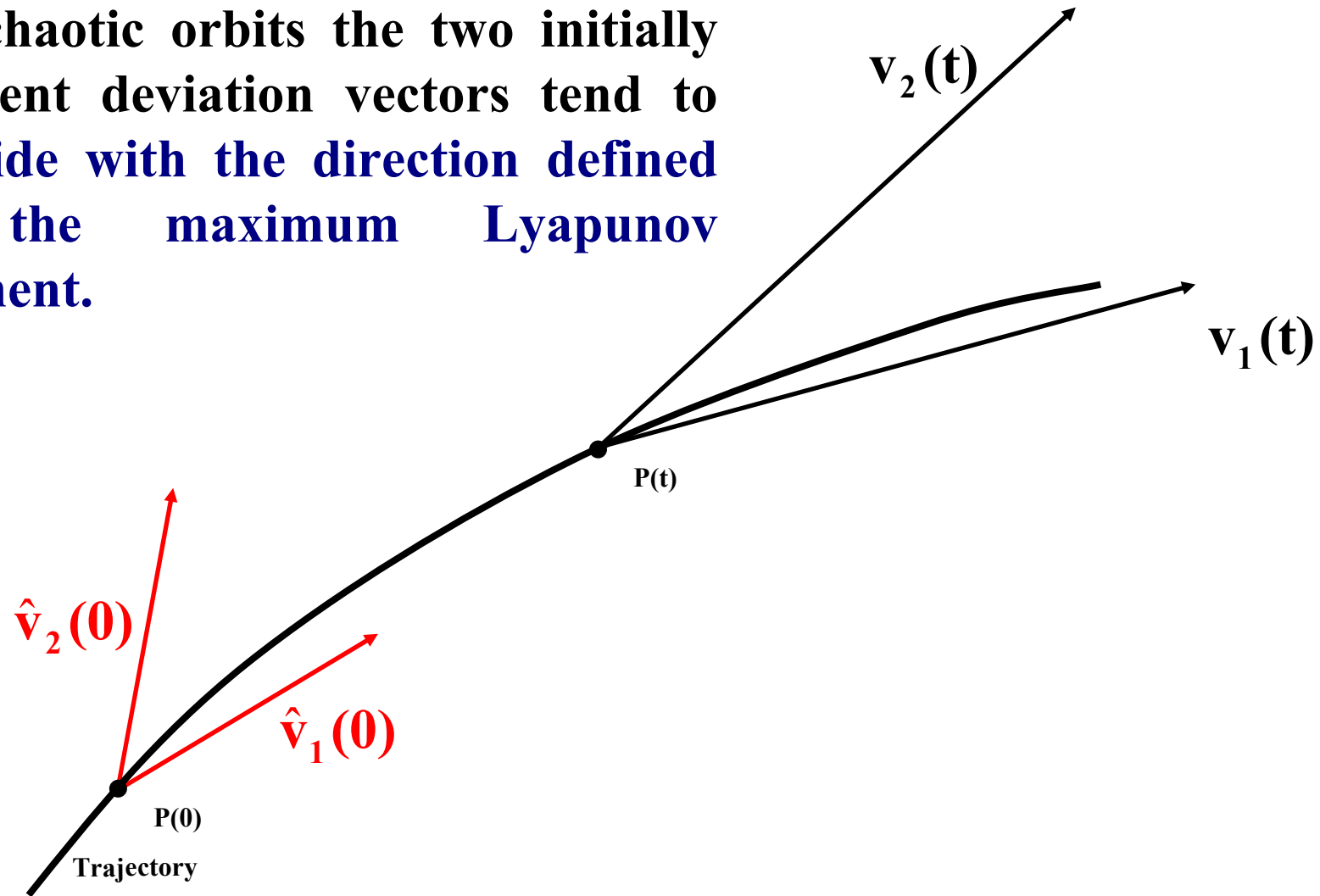
Behavior of SALI for chaotic motion

For chaotic orbits the two initially different deviation vectors tend to coincide with the direction defined by the maximum Lyapunov exponent.



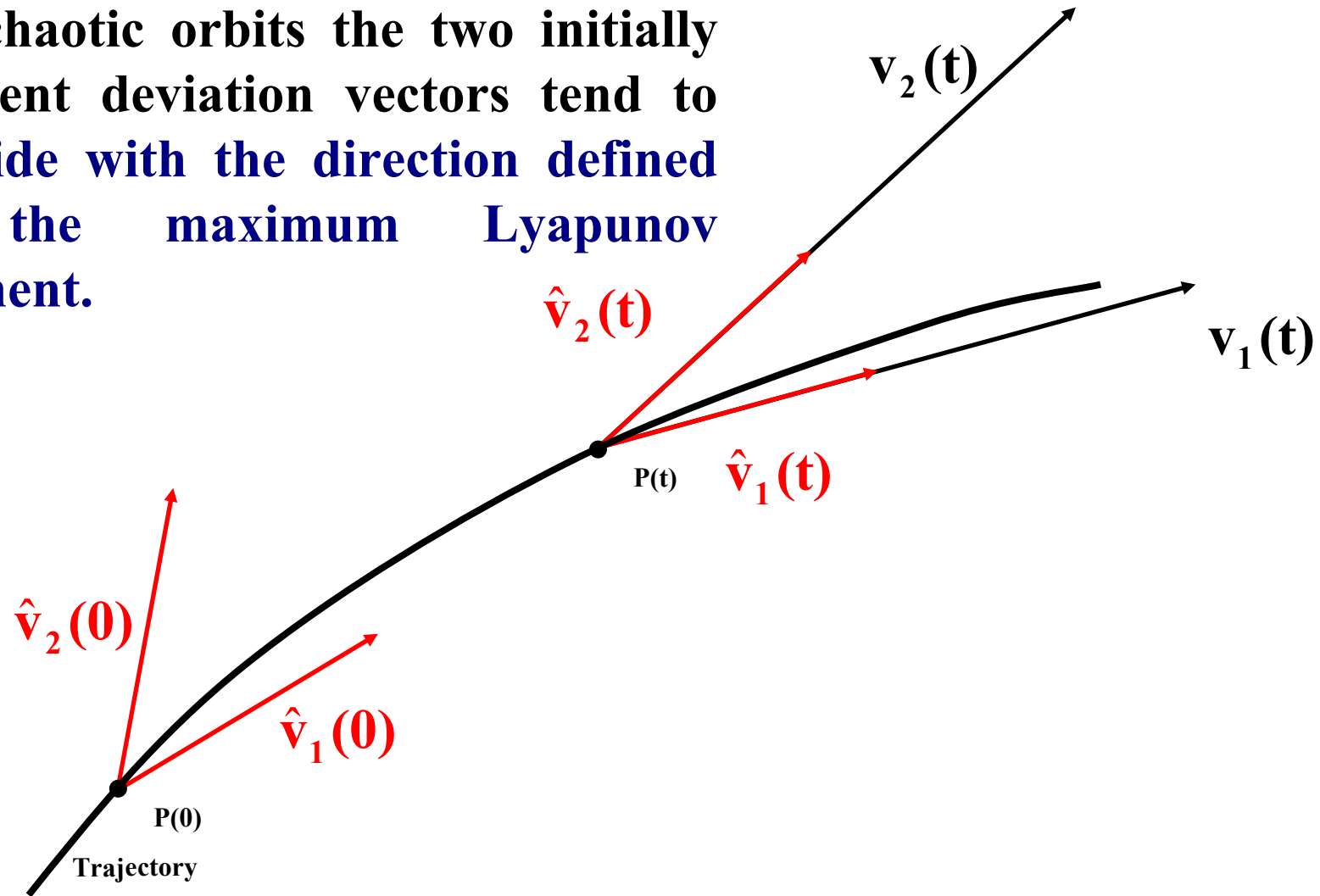
Behavior of SALI for chaotic motion

For chaotic orbits the two initially different deviation vectors tend to coincide with the direction defined by the maximum Lyapunov exponent.



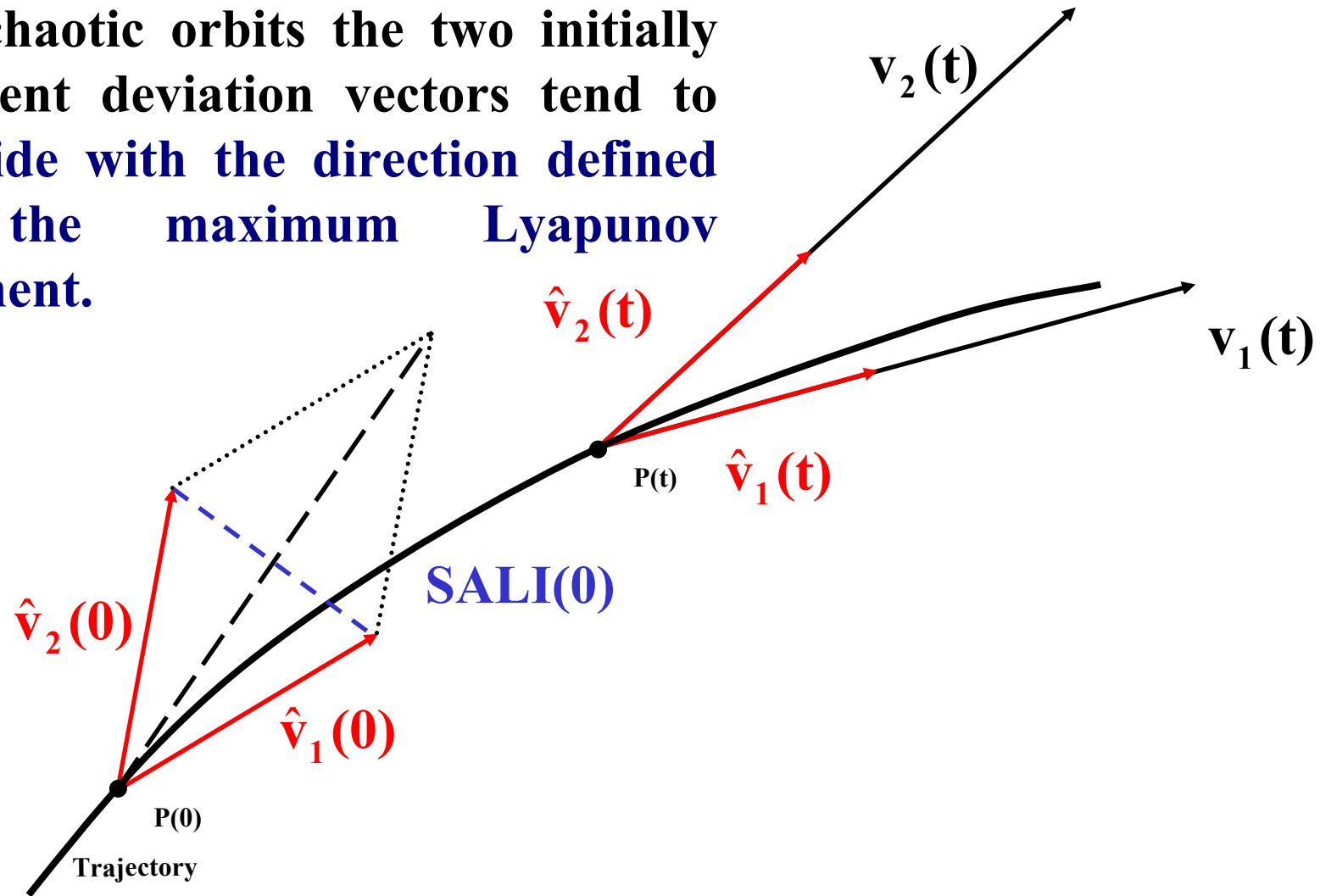
Behavior of SALI for chaotic motion

For chaotic orbits the two initially different deviation vectors tend to coincide with the direction defined by the maximum Lyapunov exponent.



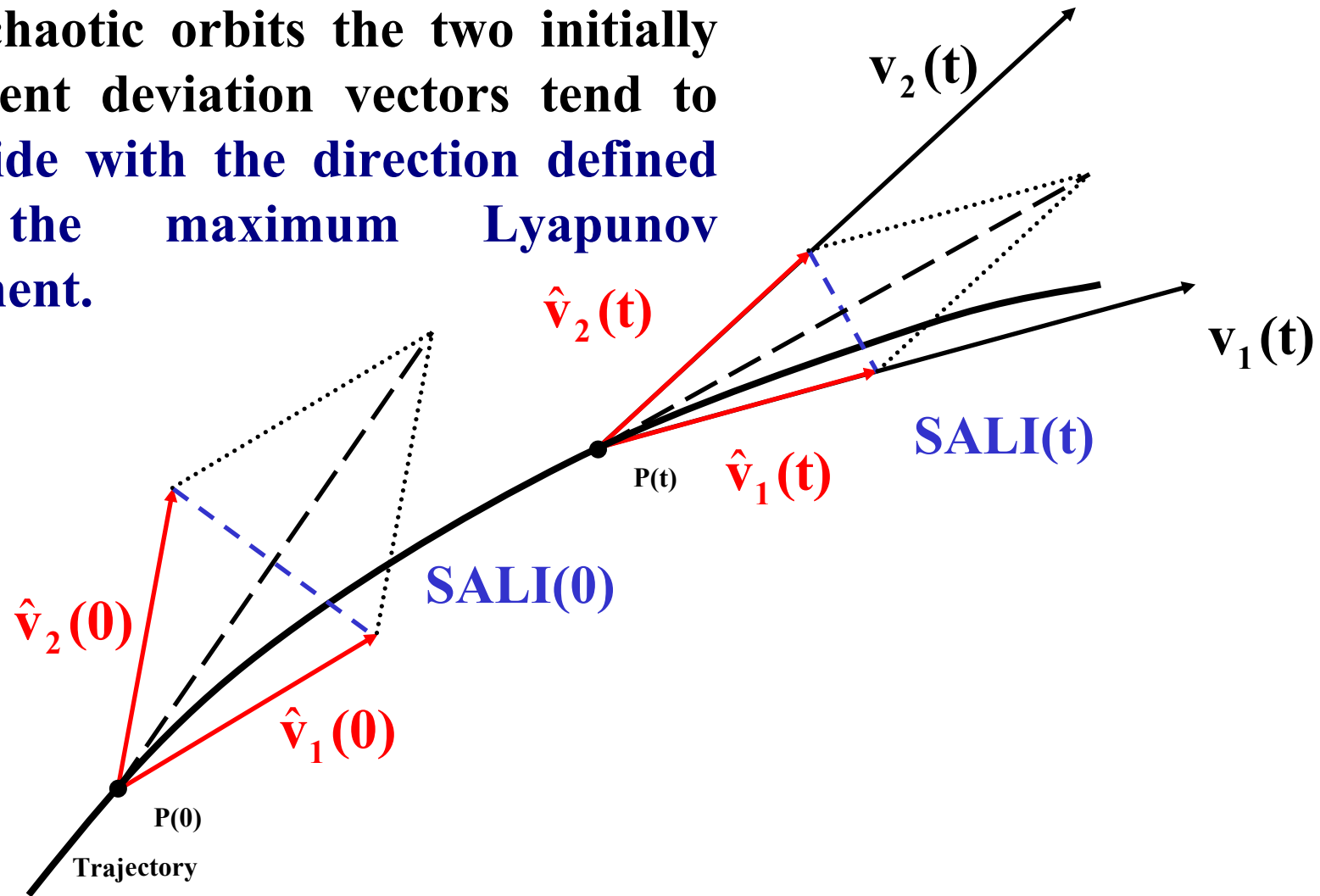
Behavior of SALI for chaotic motion

For chaotic orbits the two initially different deviation vectors tend to coincide with the direction defined by the maximum Lyapunov exponent.



Behavior of SALI for chaotic motion

For chaotic orbits the two initially different deviation vectors tend to coincide with the direction defined by the maximum Lyapunov exponent.



Behavior of SALI for chaotic motion

The evolution of a deviation vector can be approximated by:

$$\mathbf{v}_1(t) = \sum_{i=1}^n \mathbf{c}_i^{(1)} e^{\sigma_i t} \hat{\mathbf{u}}_i \approx \mathbf{c}_1^{(1)} e^{\sigma_1 t} \hat{\mathbf{u}}_1 + \mathbf{c}_2^{(1)} e^{\sigma_2 t} \hat{\mathbf{u}}_2$$

where $\sigma_1 > \sigma_2 \geq \dots \geq \sigma_n$ are the **Lyapunov exponents**. and $\hat{\mathbf{u}}_j$ $j=1, 2, \dots, 2N$ the corresponding eigendirections.

Behavior of SALI for chaotic motion

The evolution of a deviation vector can be approximated by:

$$\mathbf{v}_1(t) = \sum_{i=1}^n \mathbf{c}_i^{(1)} e^{\sigma_i t} \hat{\mathbf{u}}_i \approx \mathbf{c}_1^{(1)} e^{\sigma_1 t} \hat{\mathbf{u}}_1 + \mathbf{c}_2^{(1)} e^{\sigma_2 t} \hat{\mathbf{u}}_2$$

where $\sigma_1 > \sigma_2 \geq \dots \geq \sigma_n$ are the **Lyapunov exponents**. and $\hat{\mathbf{u}}_j$ $j=1, 2, \dots, 2N$ the corresponding eigendirections.

In this approximation, we derive a leading order estimate of the ratio

$$\frac{\mathbf{v}_1(t)}{\|\mathbf{v}_1(t)\|} \approx \frac{\mathbf{c}_1^{(1)} e^{\sigma_1 t} \hat{\mathbf{u}}_1 + \mathbf{c}_2^{(1)} e^{\sigma_2 t} \hat{\mathbf{u}}_2}{|\mathbf{c}_1^{(1)}| e^{\sigma_1 t}} = \pm \hat{\mathbf{u}}_1 + \frac{\mathbf{c}_2^{(1)}}{|\mathbf{c}_1^{(1)}|} e^{-(\sigma_1 - \sigma_2)t} \hat{\mathbf{u}}_2$$

and an analogous expression for \mathbf{v}_2

$$\frac{\mathbf{v}_2(t)}{\|\mathbf{v}_2(t)\|} \approx \frac{\mathbf{c}_1^{(2)} e^{\sigma_1 t} \hat{\mathbf{u}}_1 + \mathbf{c}_2^{(2)} e^{\sigma_2 t} \hat{\mathbf{u}}_2}{|\mathbf{c}_1^{(2)}| e^{\sigma_1 t}} = \pm \hat{\mathbf{u}}_1 + \frac{\mathbf{c}_2^{(2)}}{|\mathbf{c}_1^{(2)}|} e^{-(\sigma_1 - \sigma_2)t} \hat{\mathbf{u}}_2$$

Behavior of SALI for chaotic motion

The evolution of a deviation vector can be approximated by:

$$\mathbf{v}_1(t) = \sum_{i=1}^n \mathbf{c}_i^{(1)} e^{\sigma_i t} \hat{\mathbf{u}}_i \approx \mathbf{c}_1^{(1)} e^{\sigma_1 t} \hat{\mathbf{u}}_1 + \mathbf{c}_2^{(1)} e^{\sigma_2 t} \hat{\mathbf{u}}_2$$

where $\sigma_1 > \sigma_2 \geq \dots \geq \sigma_n$ are the **Lyapunov exponents**. and $\hat{\mathbf{u}}_j$ $j=1, 2, \dots, 2N$ the corresponding eigendirections.

In this approximation, we derive a leading order estimate of the ratio

$$\frac{\mathbf{v}_1(t)}{\|\mathbf{v}_1(t)\|} \approx \frac{\mathbf{c}_1^{(1)} e^{\sigma_1 t} \hat{\mathbf{u}}_1 + \mathbf{c}_2^{(1)} e^{\sigma_2 t} \hat{\mathbf{u}}_2}{|\mathbf{c}_1^{(1)}| e^{\sigma_1 t}} = \pm \hat{\mathbf{u}}_1 + \frac{\mathbf{c}_2^{(1)}}{|\mathbf{c}_1^{(1)}|} e^{-(\sigma_1 - \sigma_2)t} \hat{\mathbf{u}}_2$$

and an analogous expression for \mathbf{v}_2

$$\frac{\mathbf{v}_2(t)}{\|\mathbf{v}_2(t)\|} \approx \frac{\mathbf{c}_1^{(2)} e^{\sigma_1 t} \hat{\mathbf{u}}_1 + \mathbf{c}_2^{(2)} e^{\sigma_2 t} \hat{\mathbf{u}}_2}{|\mathbf{c}_1^{(2)}| e^{\sigma_1 t}} = \pm \hat{\mathbf{u}}_1 + \frac{\mathbf{c}_2^{(2)}}{|\mathbf{c}_1^{(2)}|} e^{-(\sigma_1 - \sigma_2)t} \hat{\mathbf{u}}_2$$

So we get:

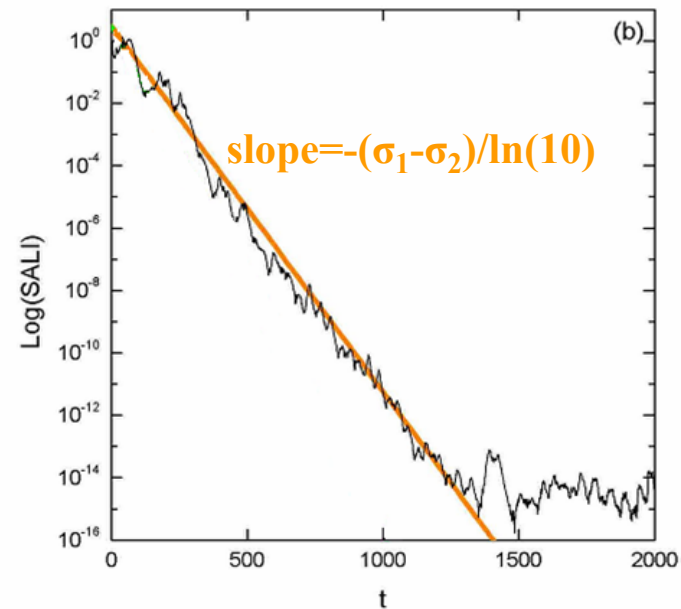
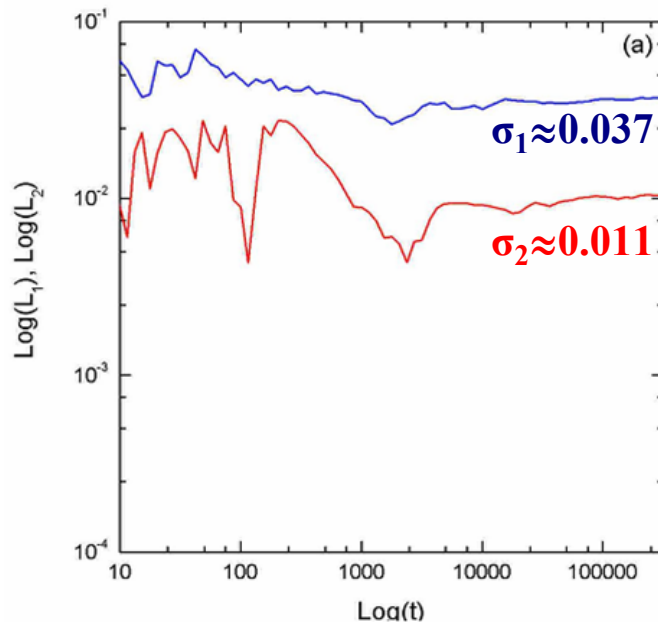
$$\text{SALI}(t) = \min \left\{ \left\| \frac{\mathbf{v}_1(t)}{\|\mathbf{v}_1(t)\|} + \frac{\mathbf{v}_2(t)}{\|\mathbf{v}_2(t)\|} \right\|, \left\| \frac{\mathbf{v}_1(t)}{\|\mathbf{v}_1(t)\|} - \frac{\mathbf{v}_2(t)}{\|\mathbf{v}_2(t)\|} \right\| \right\} \approx \left| \frac{\mathbf{c}_2^{(1)}}{|\mathbf{c}_1^{(1)}|} \pm \frac{\mathbf{c}_2^{(2)}}{|\mathbf{c}_1^{(2)}|} \right| e^{-(\sigma_1 - \sigma_2)t}$$

Behavior of SALI for chaotic motion

We test the validity of the approximation $\text{SALI} \propto e^{-(\sigma_1 - \sigma_2)t}$ (Ch.S., Antonopoulos, Bountis, Vrahatis, 2004, J. Phys. A) for a chaotic orbit of the 3D Hamiltonian

$$H = \sum_{i=1}^3 \frac{\omega_i}{2} (q_i^2 + p_i^2) + q_1^2 q_2 + q_1^2 q_3$$

with $\omega_1=1$, $\omega_2=1.4142$, $\omega_3=1.7321$, $H=0.09$

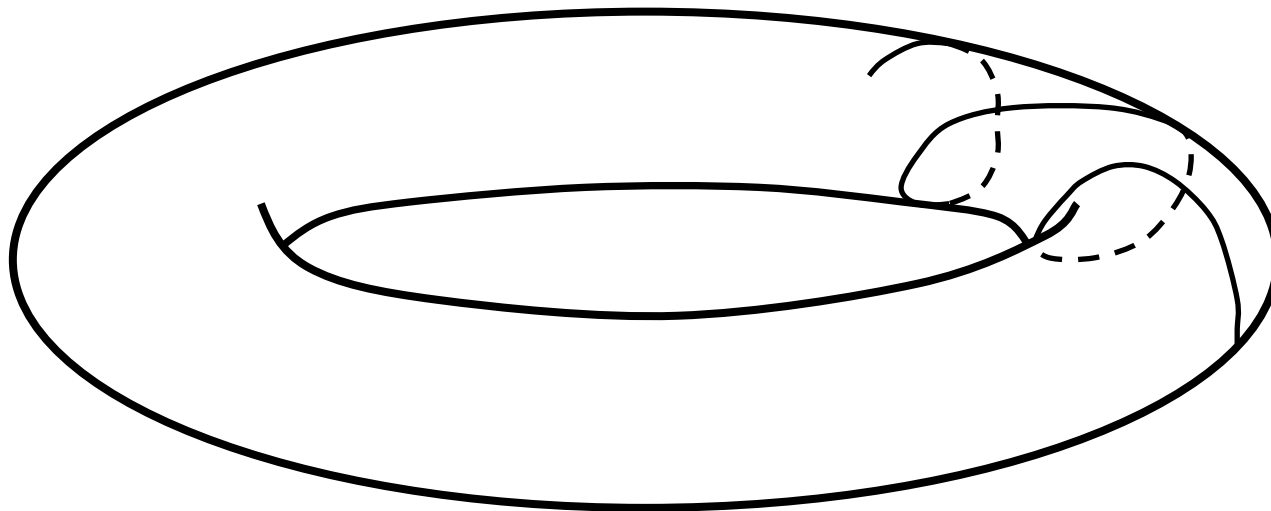


Behavior of SALI for regular motion

Regular motion occurs on a torus and two different initial deviation vectors become tangent to the torus, generally having different directions.

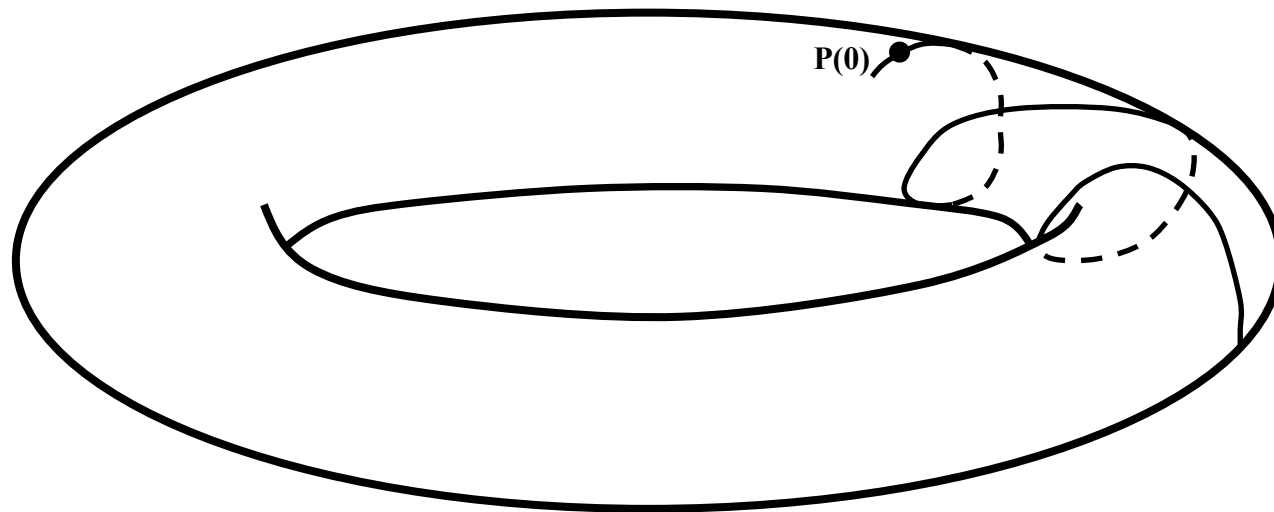
Behavior of SALI for **regular motion**

Regular motion occurs on a torus and two different initial deviation vectors **become tangent to the torus, generally having different directions.**



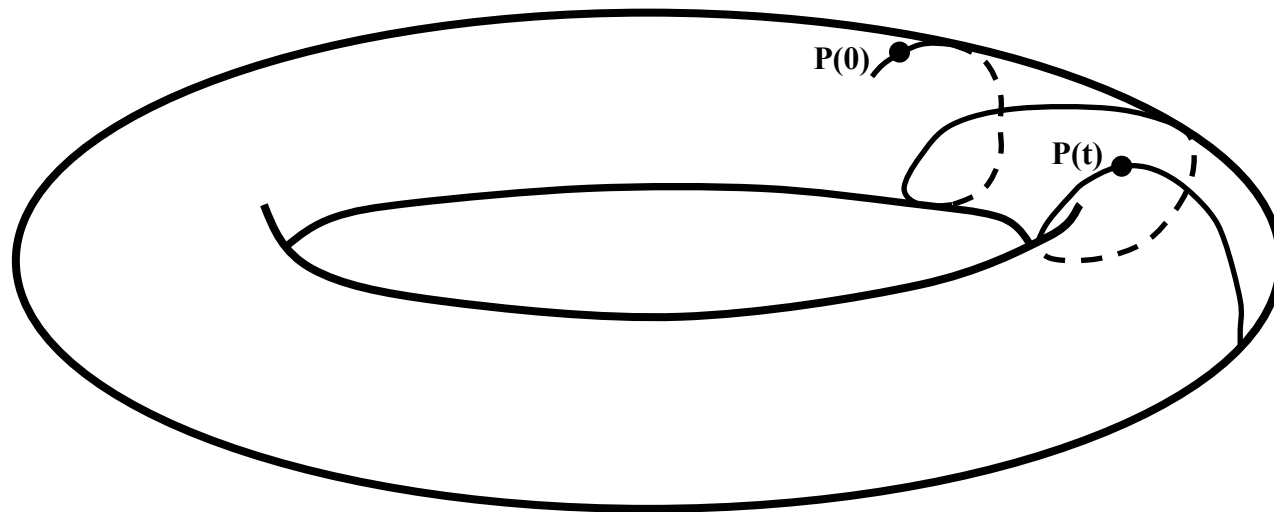
Behavior of SALI for **regular motion**

Regular motion occurs on a torus and two different initial deviation vectors **become tangent to the torus, generally having different directions.**



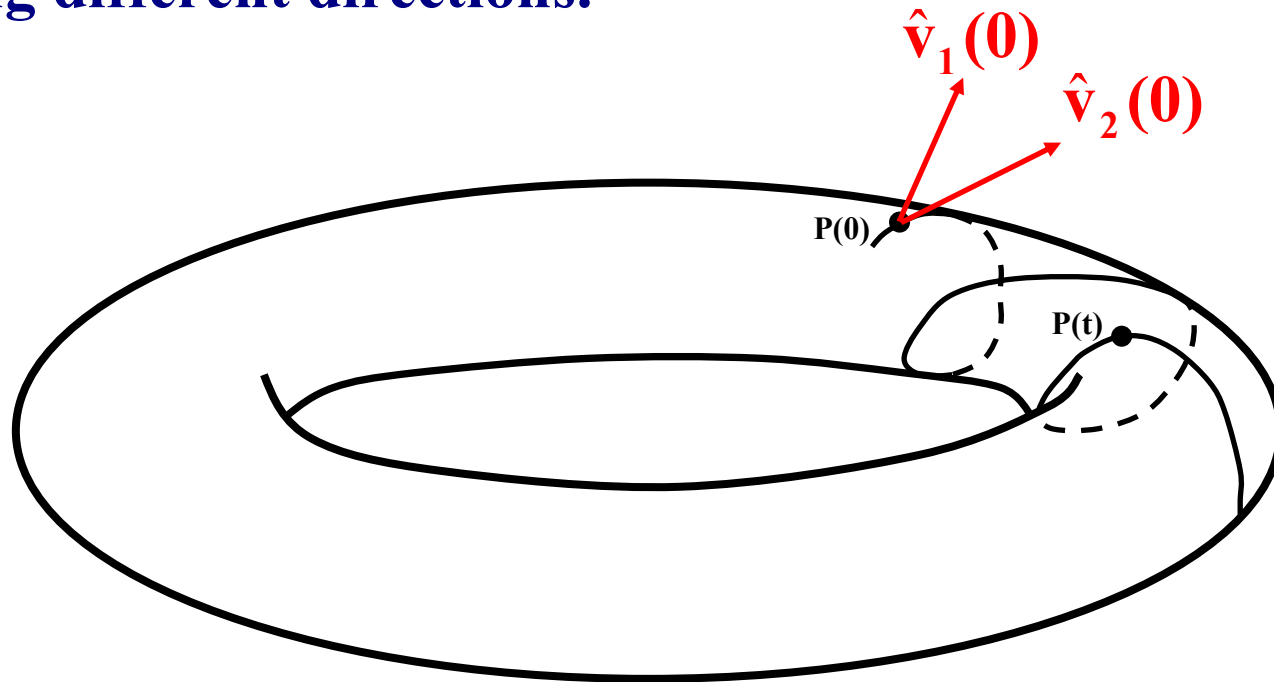
Behavior of SALI for **regular motion**

Regular motion occurs on a torus and two different initial deviation vectors **become tangent to the torus, generally having different directions.**



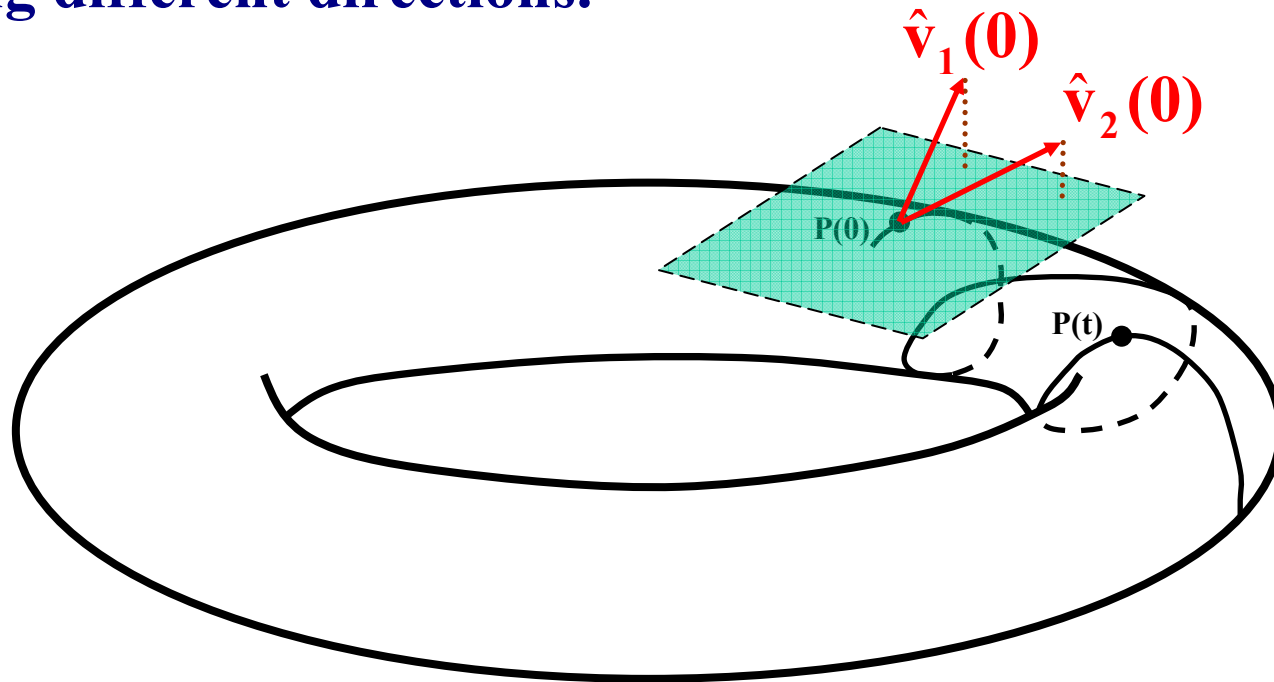
Behavior of SALI for **regular motion**

Regular motion occurs on a torus and two different initial deviation vectors **become tangent to the torus, generally having different directions.**



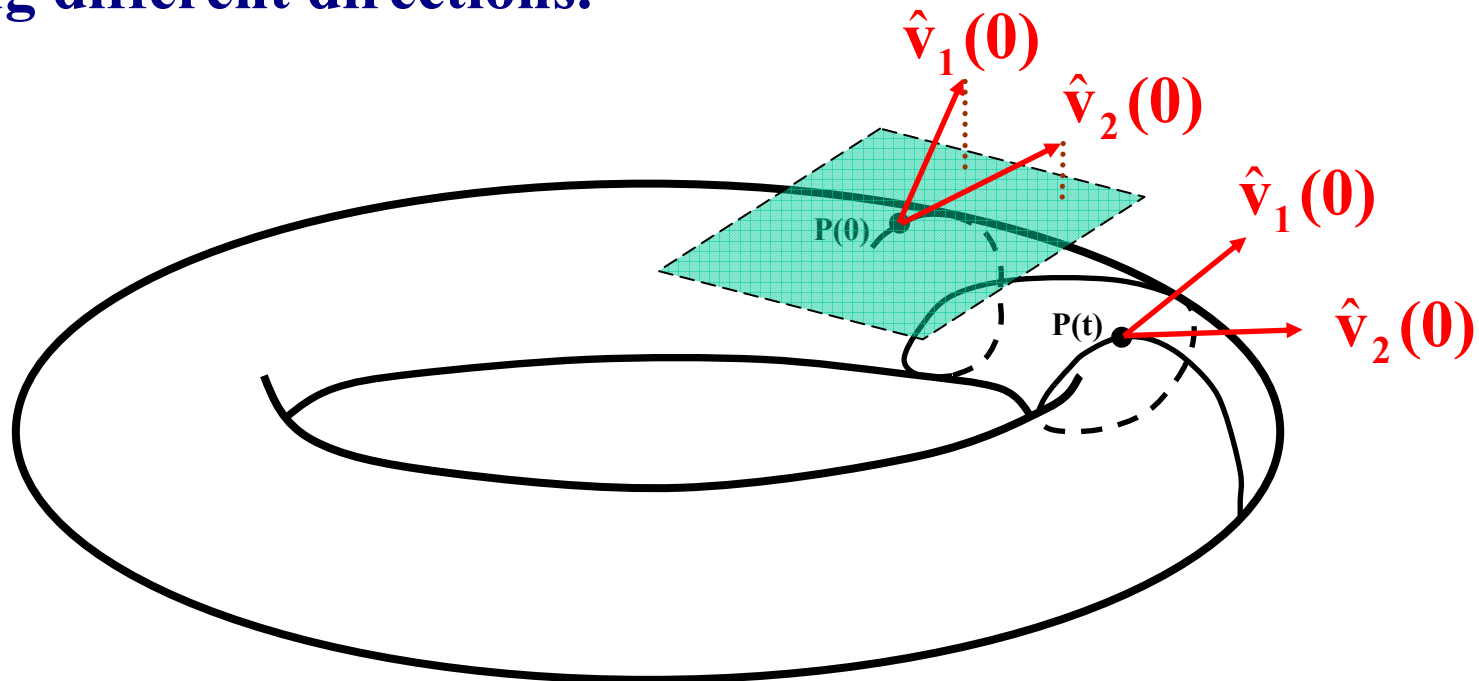
Behavior of SALI for **regular motion**

Regular motion occurs on a torus and two different initial deviation vectors **become tangent to the torus, generally having different directions.**



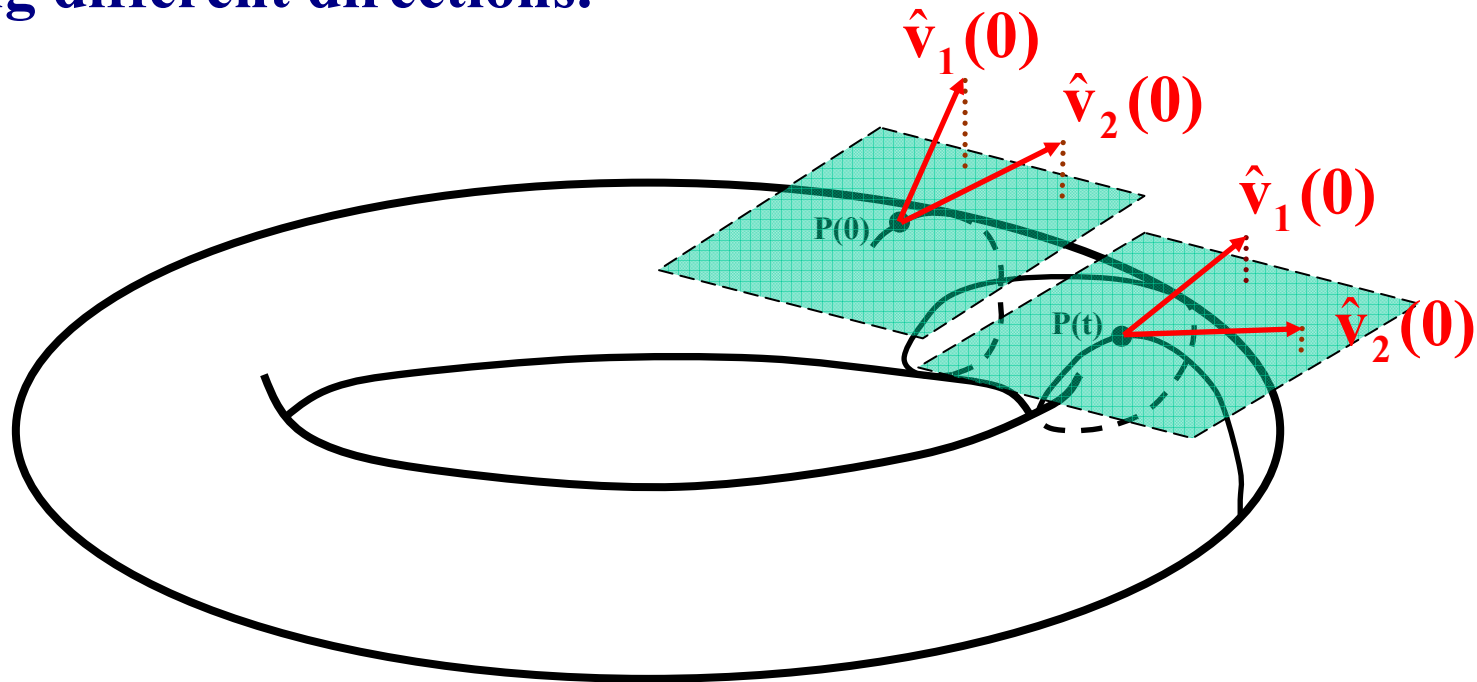
Behavior of SALI for **regular motion**

Regular motion occurs on a torus and two different initial deviation vectors **become tangent to the torus**, generally **having different directions**.



Behavior of SALI for **regular motion**

Regular motion occurs on a torus and two different initial deviation vectors **become tangent to the torus, generally having different directions.**



Applications – Hénon-Heiles system

As an example, we consider the 2D Hénon-Heiles system:

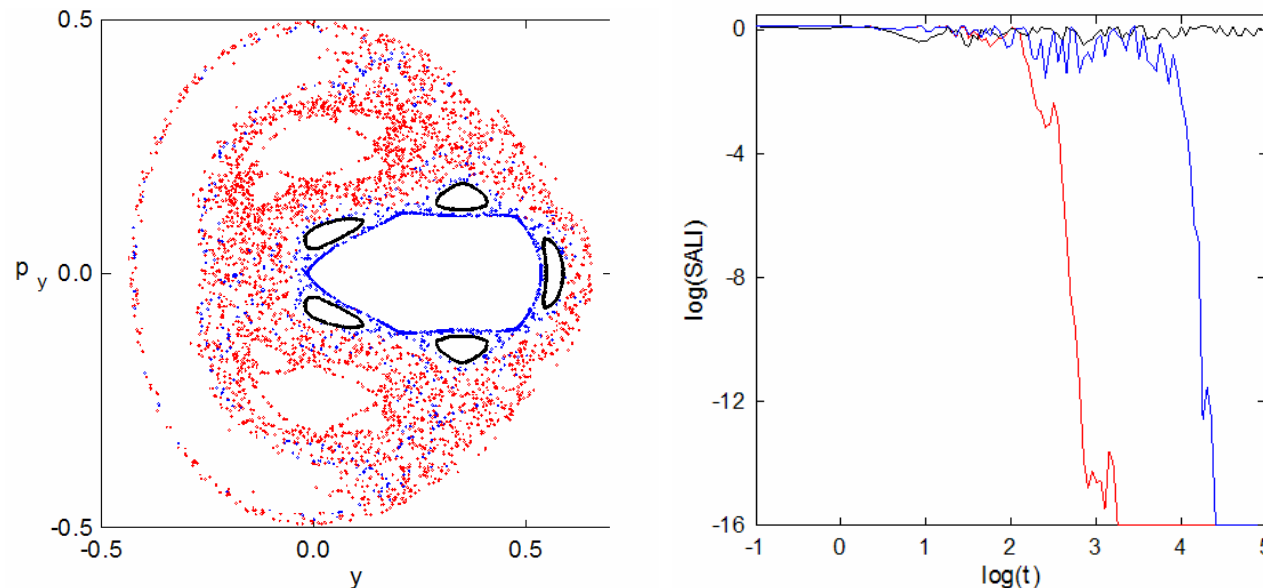
$$H_2 = \frac{1}{2}(p_x^2 + p_y^2) + \frac{1}{2}(x^2 + y^2) + x^2y - \frac{1}{3}y^3$$

For $E=1/8$ we consider the orbits with initial conditions:

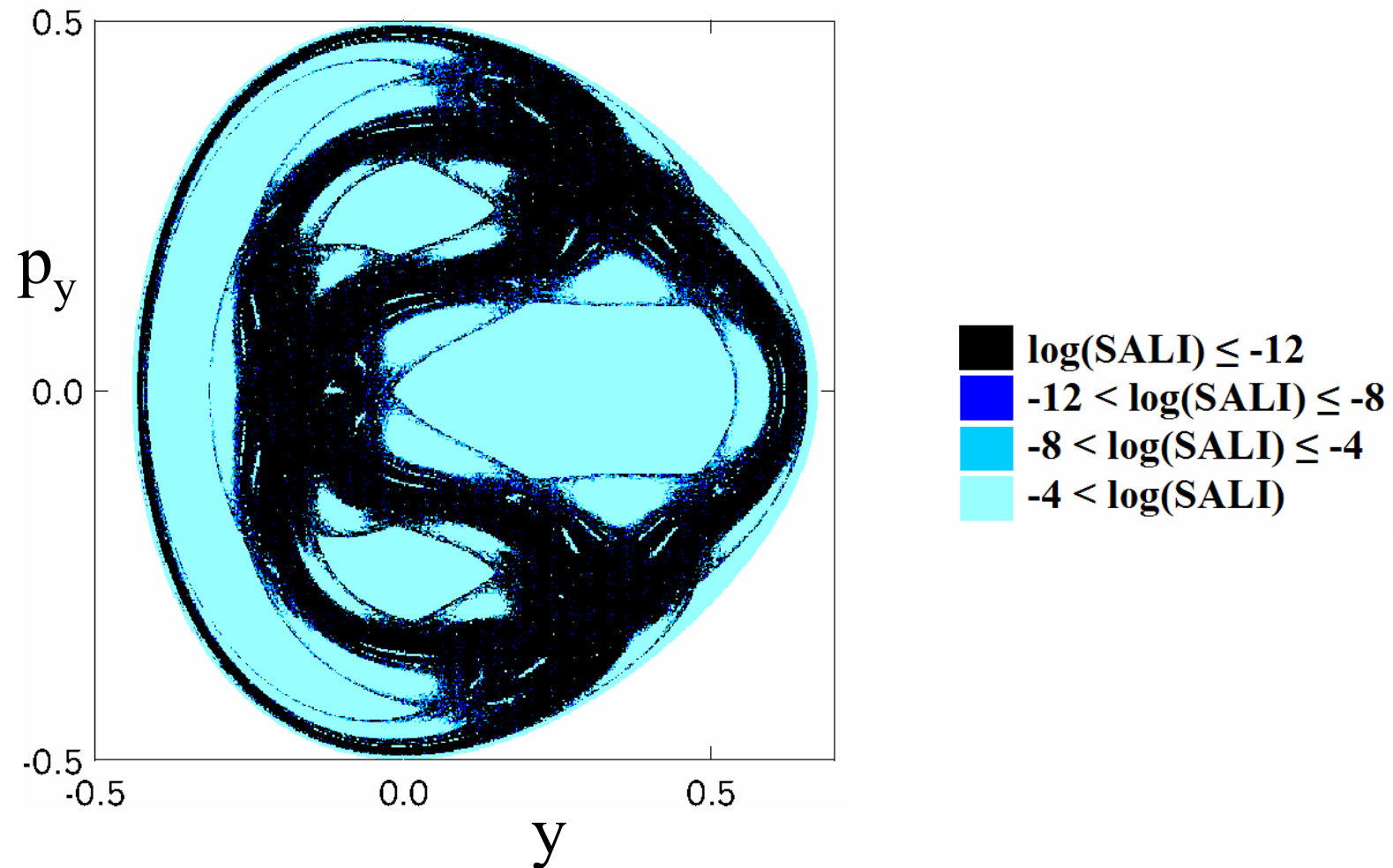
Regular orbit, $x=0$, $y=0.55$, $p_x=0.2417$, $p_y=0$

Chaotic orbit, $x=0$, $y=-0.016$, $p_x=0.49974$, $p_y=0$

Chaotic orbit, $x=0$, $y=-0.01344$, $p_x=0.49982$, $p_y=0$



Applications – Hénon-Heiles system



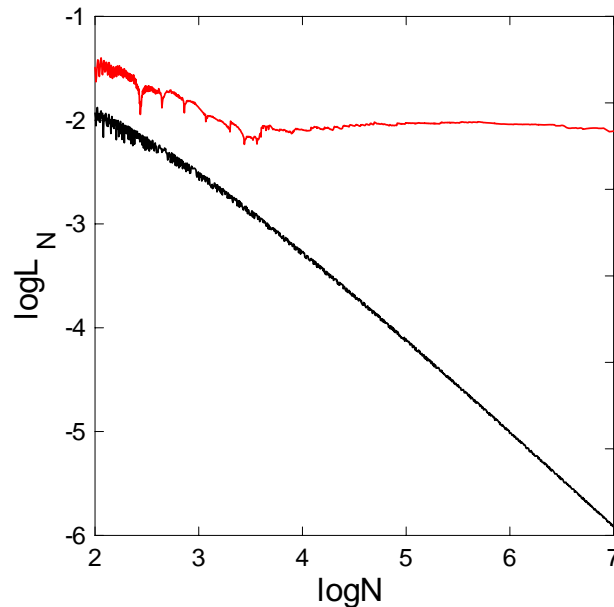
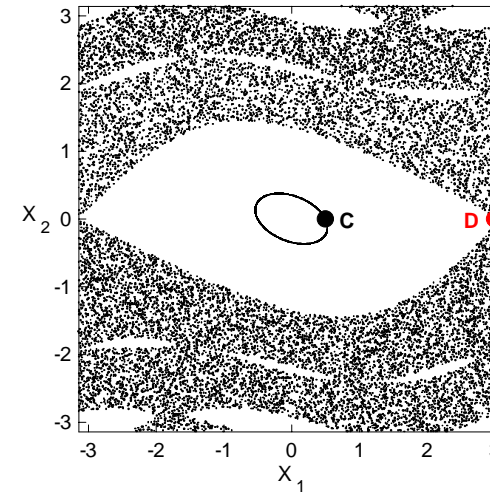
Applications – 4D map

$$\begin{aligned}
 x'_1 &= x_1 + x_2 \\
 x'_2 &= x_2 - v \sin(x_1 + x_2) - \mu [1 - \cos(x_1 + x_2 + x_3 + x_4)] \\
 x'_3 &= x_3 + x_4 \\
 x'_4 &= x_4 - \kappa \sin(x_3 + x_4) - \mu [1 - \cos(x_1 + x_2 + x_3 + x_4)]
 \end{aligned} \pmod{2\pi}$$

For $v=0.5$, $\kappa=0.1$, $\mu=0.1$ we consider the orbits:

regular orbit C with initial conditions $x_1=0.5$, $x_2=0$, $x_3=0.5$, $x_4=0$.

chaotic orbit D with initial conditions $x_1=3$, $x_2=0$, $x_3=0.5$, $x_4=0$.



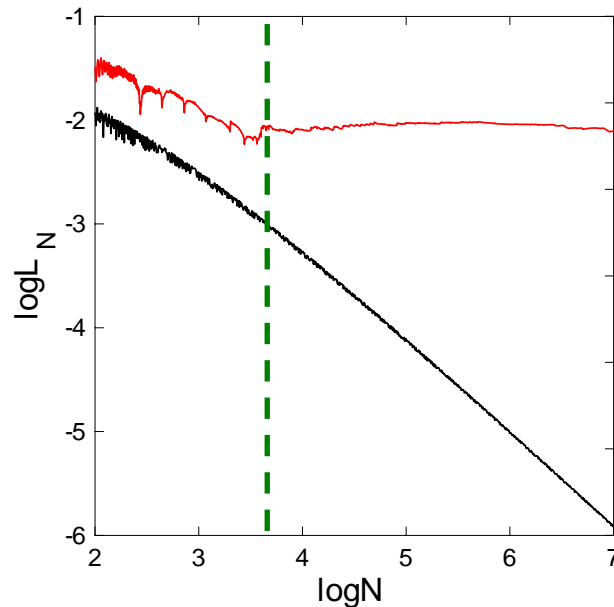
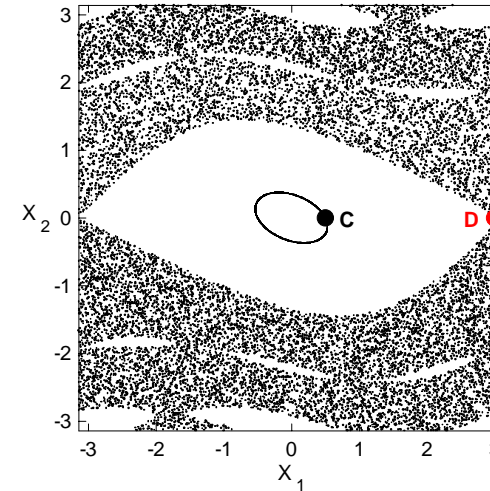
Applications – 4D map

$$\begin{aligned}
 x_1' &= x_1 + x_2 \\
 x_2' &= x_2 - v \sin(x_1 + x_2) - \mu [1 - \cos(x_1 + x_2 + x_3 + x_4)] \\
 x_3' &= x_3 + x_4 \\
 x_4' &= x_4 - \kappa \sin(x_3 + x_4) - \mu [1 - \cos(x_1 + x_2 + x_3 + x_4)]
 \end{aligned} \pmod{2\pi}$$

For $v=0.5$, $\kappa=0.1$, $\mu=0.1$ we consider the orbits:

regular orbit C with initial conditions $x_1=0.5$, $x_2=0$, $x_3=0.5$, $x_4=0$.

chaotic orbit D with initial conditions $x_1=3$, $x_2=0$, $x_3=0.5$, $x_4=0$.



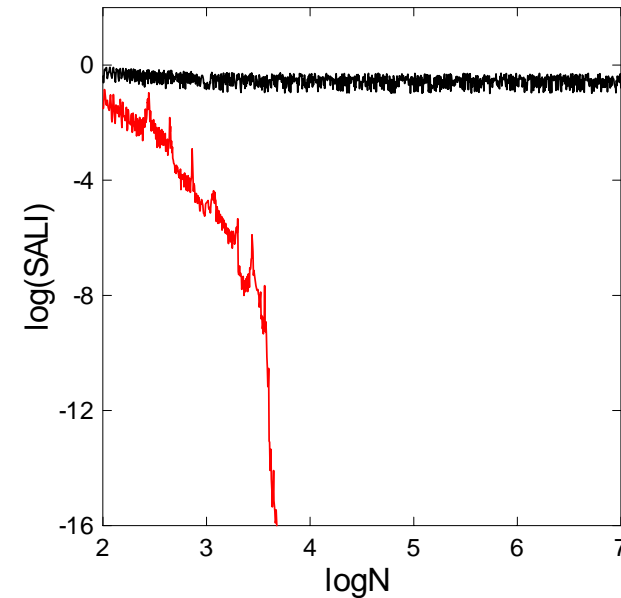
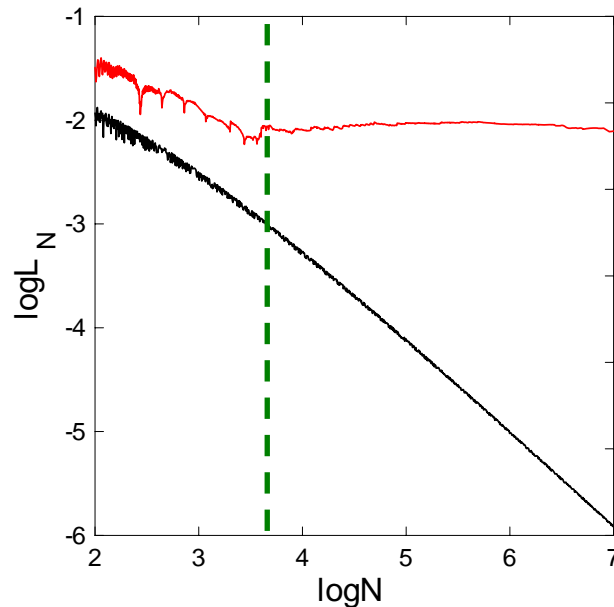
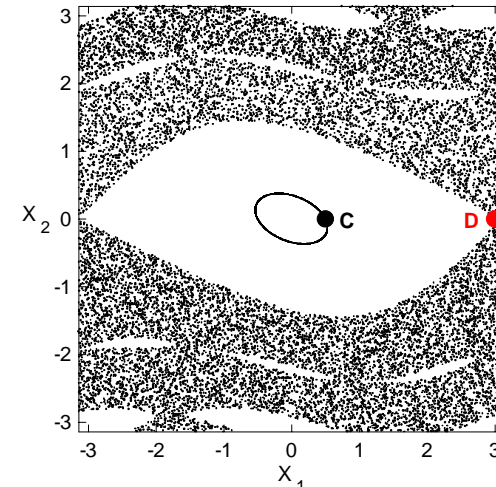
Applications – 4D map

$$\begin{aligned}
 x_1' &= x_1 + x_2 \\
 x_2' &= x_2 - \nu \sin(x_1 + x_2) - \mu [1 - \cos(x_1 + x_2 + x_3 + x_4)] \\
 x_3' &= x_3 + x_4 \\
 x_4' &= x_4 - \kappa \sin(x_3 + x_4) - \mu [1 - \cos(x_1 + x_2 + x_3 + x_4)]
 \end{aligned} \pmod{2\pi}$$

For $\nu=0.5$, $\kappa=0.1$, $\mu=0.1$ we consider the orbits:

regular orbit C with initial conditions $x_1=0.5$, $x_2=0$, $x_3=0.5$, $x_4=0$.

chaotic orbit D with initial conditions $x_1=3$, $x_2=0$, $x_3=0.5$, $x_4=0$.



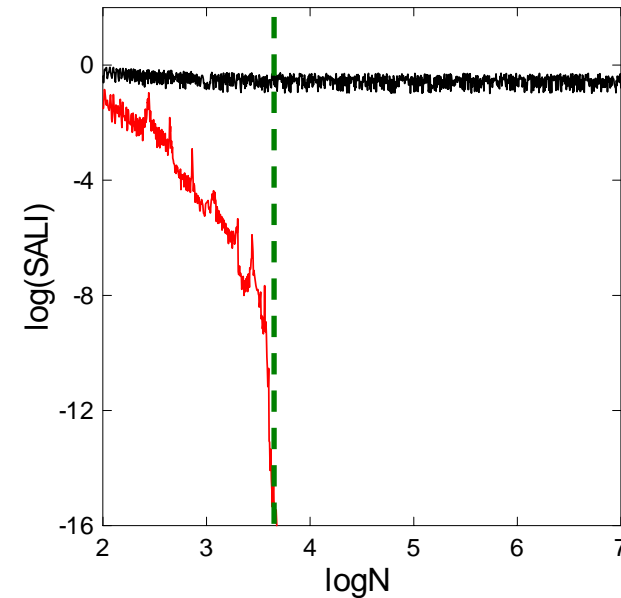
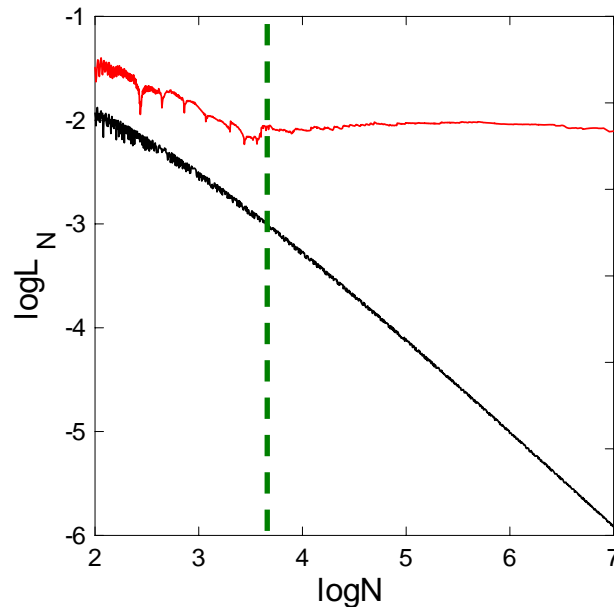
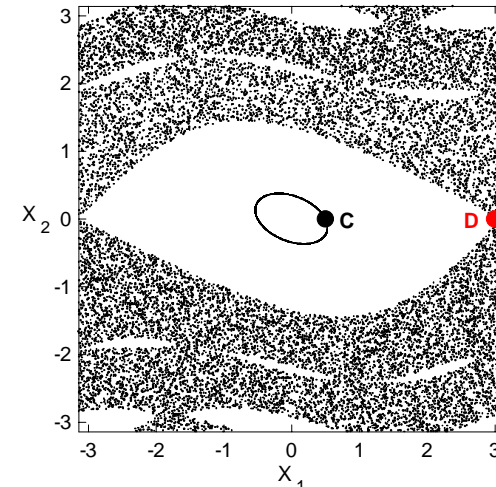
Applications – 4D map

$$\begin{aligned}x'_1 &= x_1 + x_2 \\x'_2 &= x_2 - \nu \sin(x_1 + x_2) - \mu [1 - \cos(x_1 + x_2 + x_3 + x_4)] \\x'_3 &= x_3 + x_4 \\x'_4 &= x_4 - \kappa \sin(x_3 + x_4) - \mu [1 - \cos(x_1 + x_2 + x_3 + x_4)]\end{aligned} \quad (\text{mod } 2\pi)$$

For $\nu=0.5$, $\kappa=0.1$, $\mu=0.1$ we consider the orbits:

regular orbit C with initial conditions $x_1=0.5$, $x_2=0$, $x_3=0.5$, $x_4=0$.

chaotic orbit D with initial conditions $x_1=3$, $x_2=0$, $x_3=0.5$, $x_4=0$.



Applications – 4D Accelerator map

We consider the 4D symplectic map

$$\begin{pmatrix} x'_1 \\ x'_2 \\ x'_3 \\ x'_4 \end{pmatrix} = \begin{pmatrix} \cos\omega_1 & -\sin\omega_1 & 0 & 0 \\ \sin\omega_1 & \cos\omega_1 & 0 & 0 \\ 0 & 0 & \cos\omega_2 & -\sin\omega_2 \\ 0 & 0 & \sin\omega_2 & \cos\omega_2 \end{pmatrix} \times \begin{pmatrix} x_1 \\ x_2 + x_1^2 - x_3^2 \\ x_3 \\ x_4 - 2x_1x_3 \end{pmatrix}$$

describing the **instantaneous sextupole ‘kicks’** experienced by a particle as it passes through an accelerator (Turchetti & Scandale 1991, Bountis & Tompaidis 1991, Vrahatis et al. 1996, 1997).

x_1 and x_3 are the particle’s deflections from the ideal circular orbit, in the horizontal and vertical directions respectively.

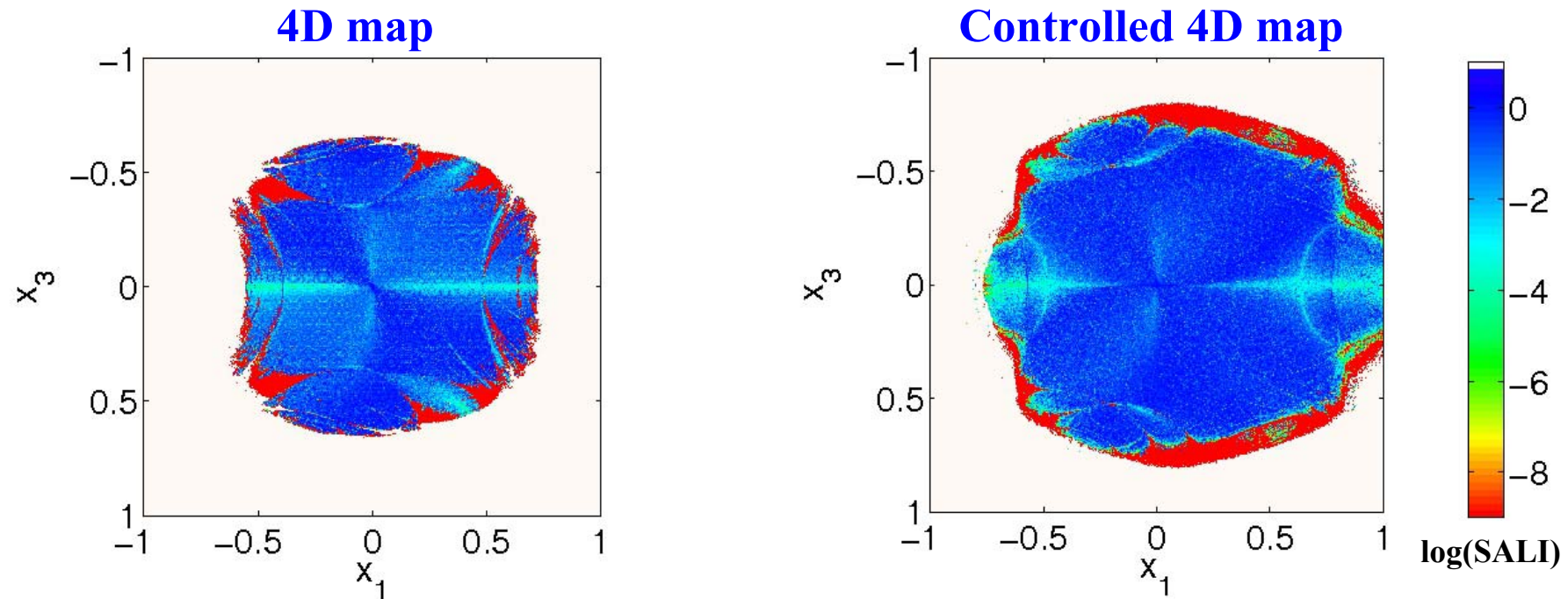
x_2 and x_4 are the associated momenta

ω_1, ω_2 are related to the accelerator’s tunes q_x, q_y by $\omega_1=2\pi q_x, \omega_2=2\pi q_y$

Our goal is to estimate the **region of stability** of the particle’s motion, the so-called **dynamic aperture** of the beam (Bountis, Ch.S., 2006, Nucl. Inst Meth. Phys Res. A) and to increase its size using chaos control techniques (Boreaux, Carletti, Ch.S., Vittot, 2011, acc-ph/1007.1562, Boreaux, Carletti, Ch.S., Papaphilippou, Vittot, 2011, acc-ph/1103.5631).

4D Accelerator map – "Global" study

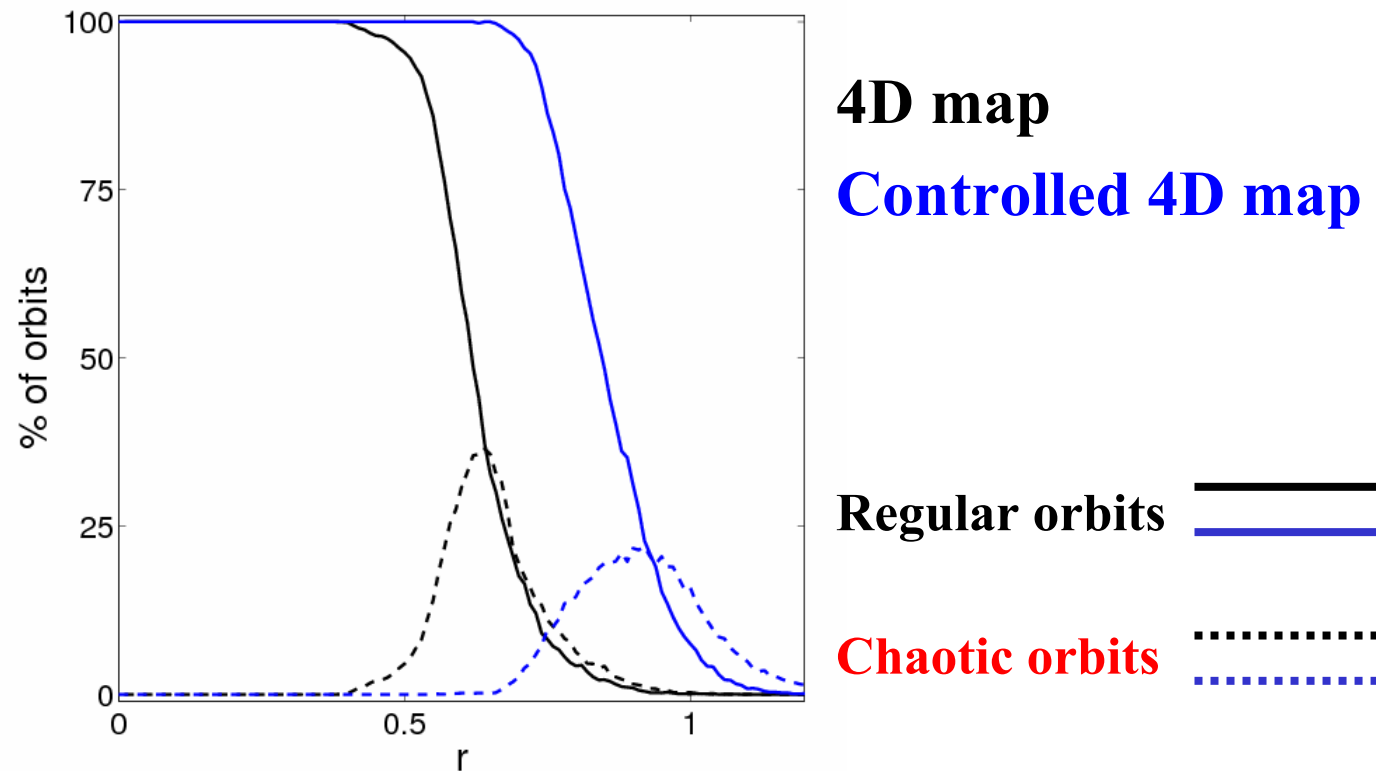
Regions of **different values of the SALI** on the subspace $x_2(0)=x_4(0)=0$, after 10^5 iterations ($q_x=0.61803$ $q_y=0.4152$)



4D Accelerator map – "Global" study

Increase of the dynamic aperture

We evolve many orbits in 4D hyperspheres of radius r centered at $x_1=x_2=x_3=x_4=0$, for 10^5 iterations.



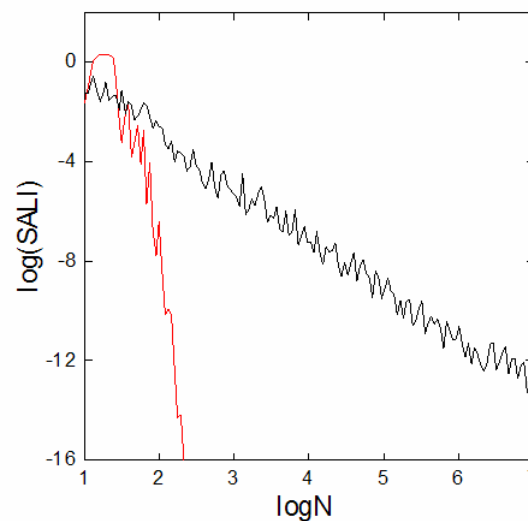
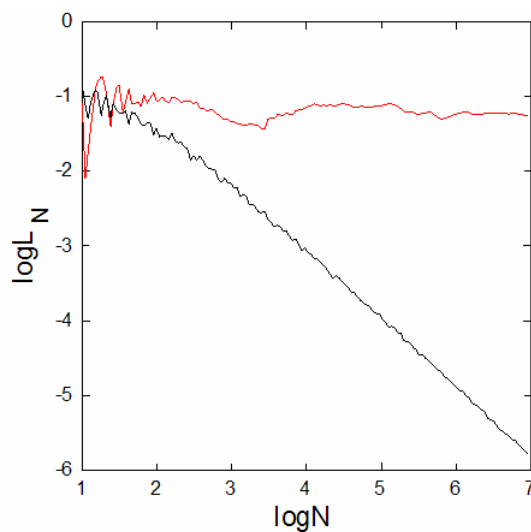
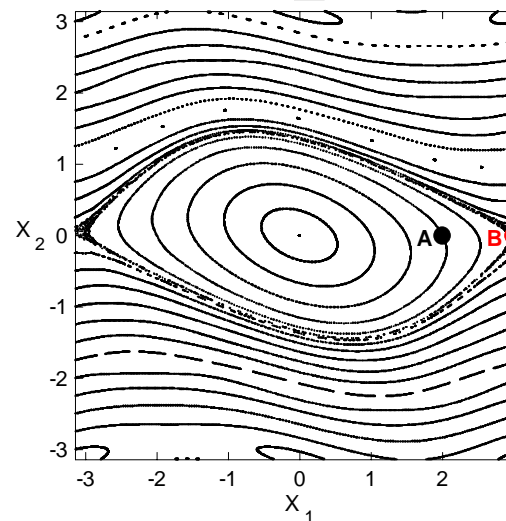
Applications – 2D map

$$\begin{aligned}x_1' &= x_1 + x_2 \\x_2' &= x_2 - v \sin(x_1 + x_2)\end{aligned}\quad (\text{mod } 2\pi)$$

For $v=0.5$ we consider the orbits:

regular orbit A with initial conditions $x_1=2, x_2=0$.

chaotic orbit B with initial conditions $x_1=3, x_2=0$.



Behavior of SALI

2D maps

SALI $\rightarrow 0$ both for regular and chaotic orbits

following, however, completely different time rates which allows us to distinguish between the two cases.

Hamiltonian flows and multidimensional maps

SALI $\rightarrow 0$ for chaotic orbits

SALI $\rightarrow \text{constant} \neq 0$ for regular orbits

Questions

Can we generalize SALI so that the new index:

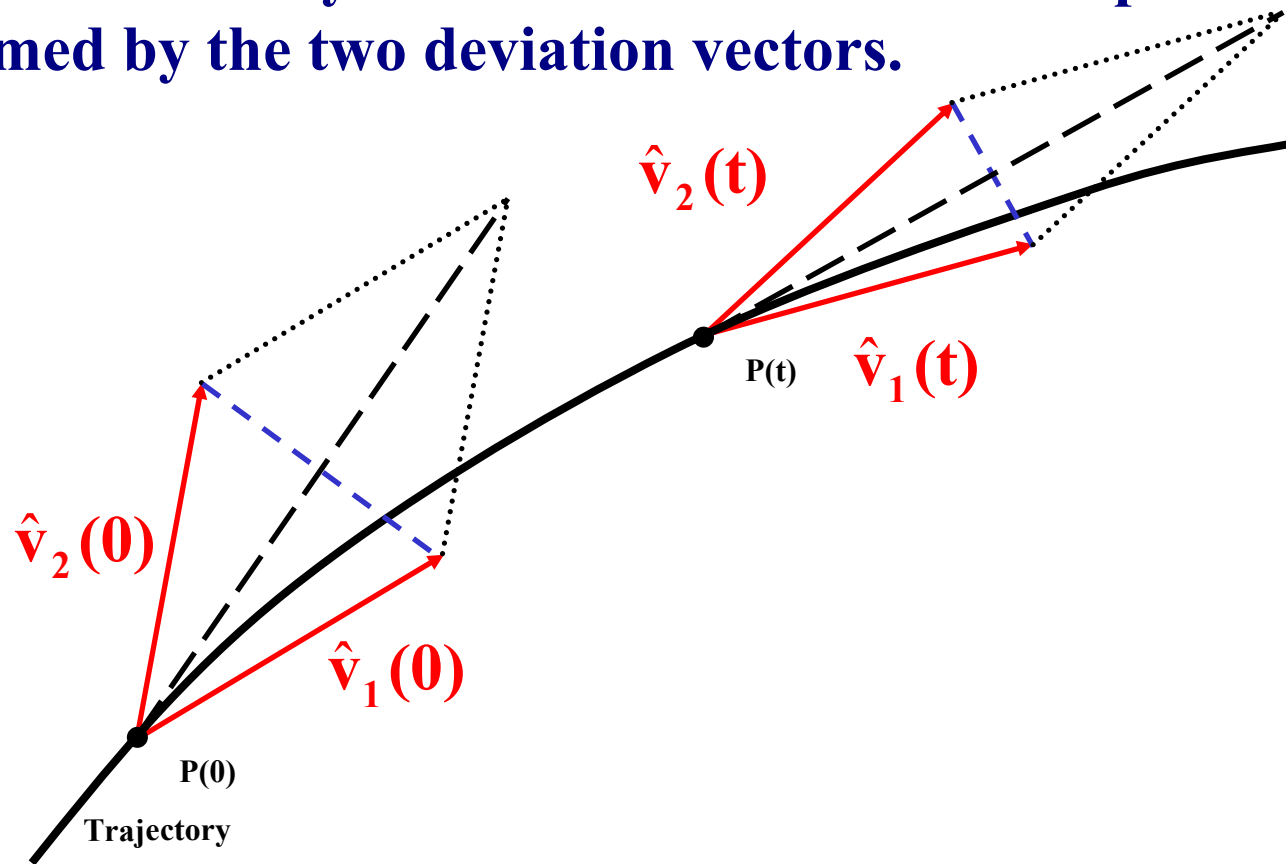
- Can rapidly reveal the nature of chaotic orbits with $\sigma_1 \approx \sigma_2$ ($\text{SALI} \propto e^{-(\sigma_1 - \sigma_2)t}$)?
- Depends on several Lyapunov exponents for chaotic orbits?
- Exhibits power-law decay for regular orbits depending on the dimensionality of the tangent space of the reference orbit as for 2D maps?

Definition of Generalized Alignment Index (GALI)

SALI effectively measures the ‘area’ of the parallelogram formed by the two deviation vectors.

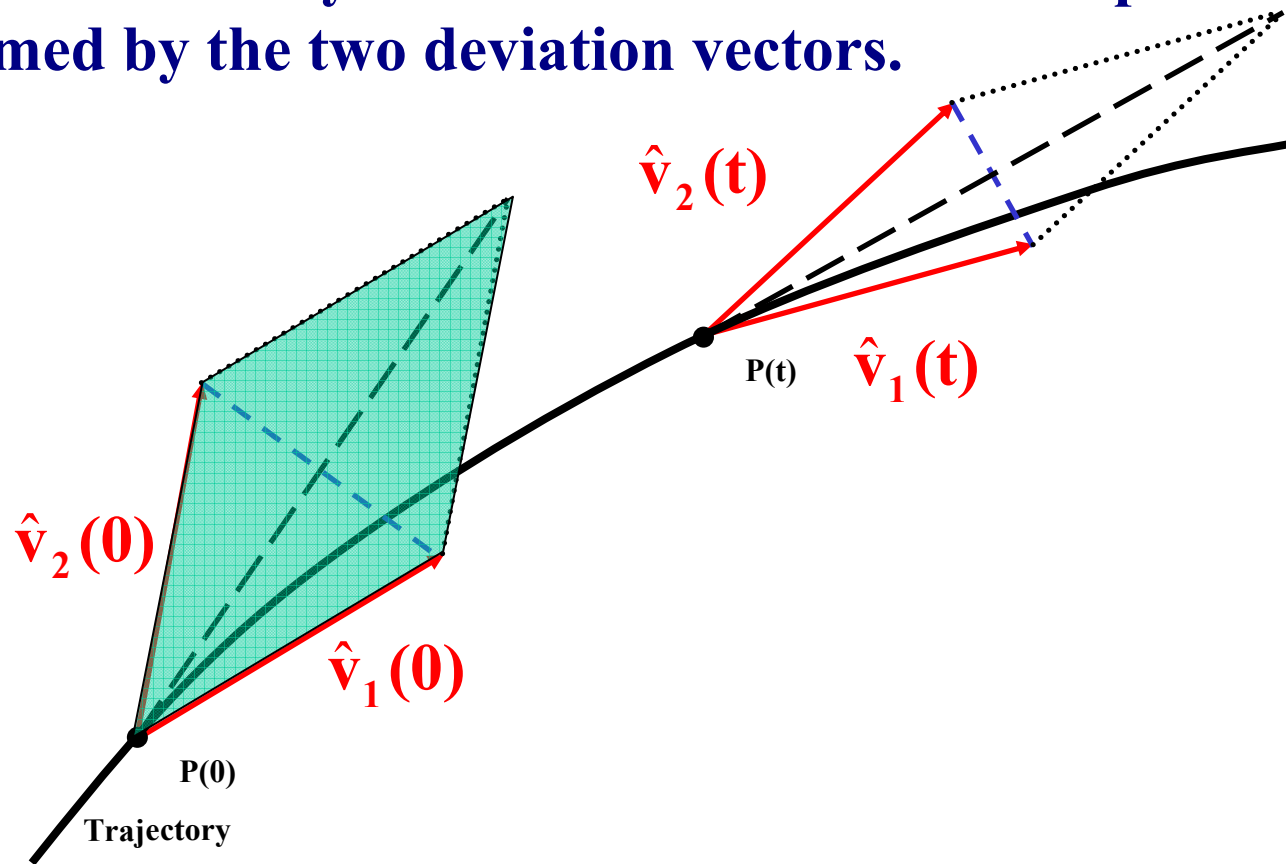
Definition of Generalized Alignment Index (GALI)

SALI effectively measures the ‘area’ of the parallelogram formed by the two deviation vectors.



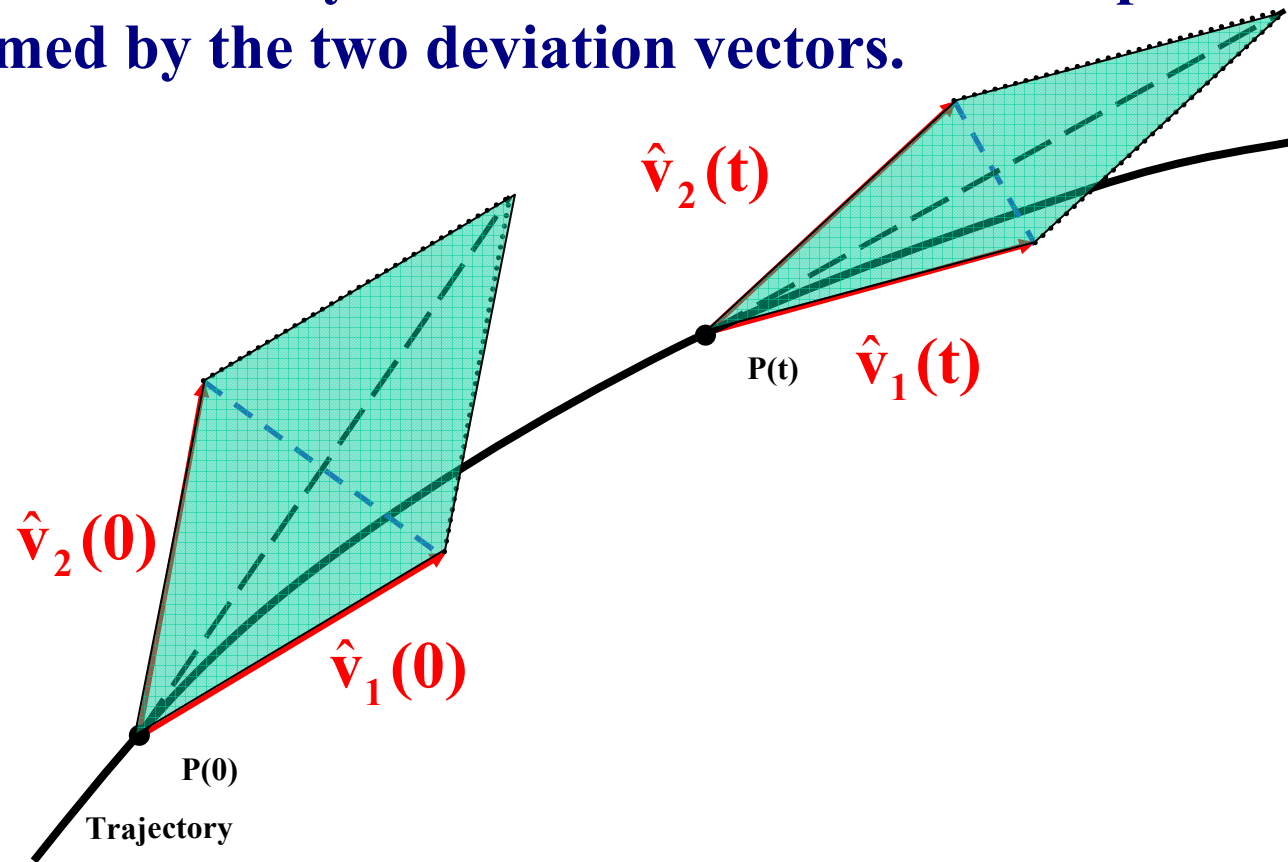
Definition of Generalized Alignment Index (GALI)

SALI effectively measures the ‘area’ of the parallelogram formed by the two deviation vectors.



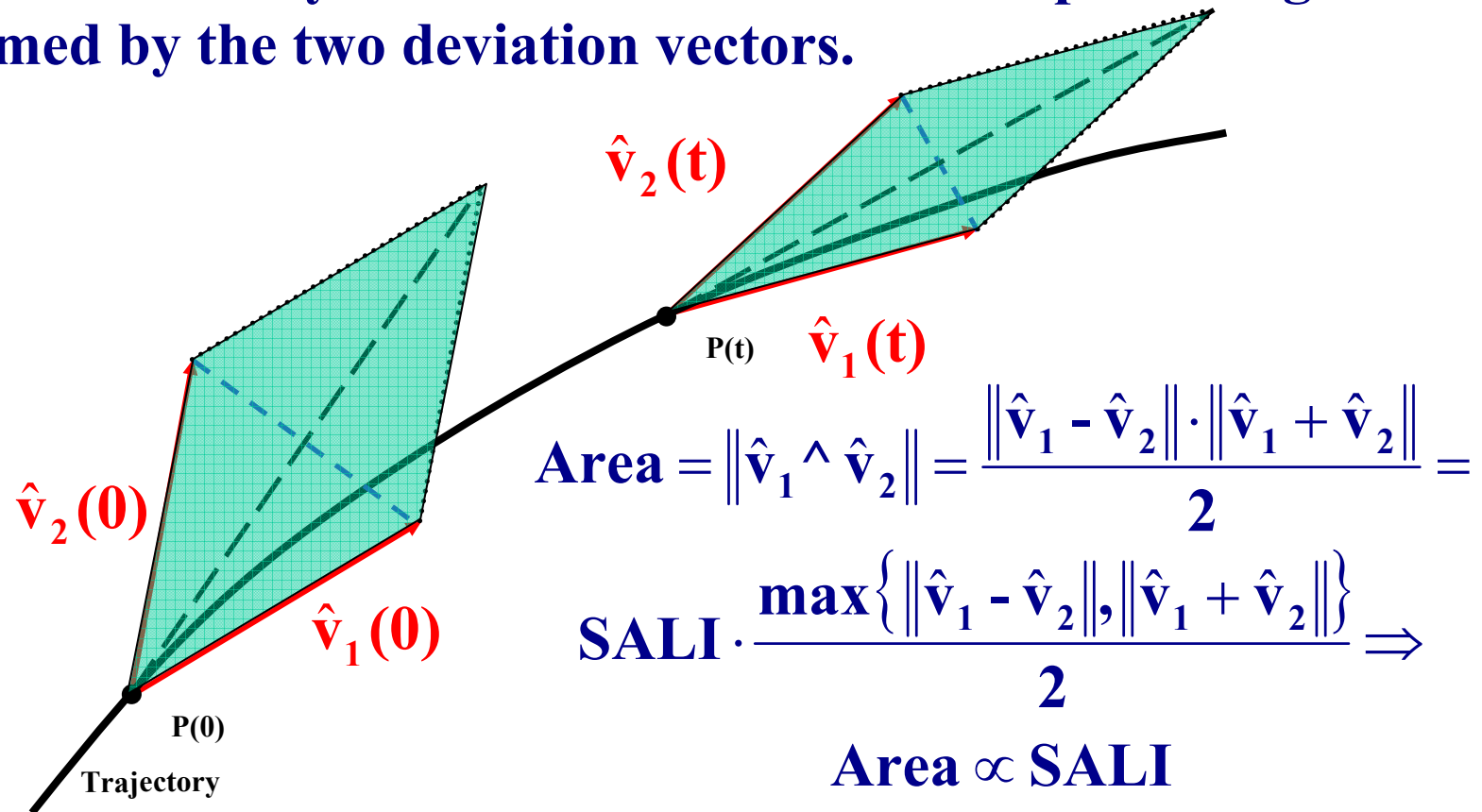
Definition of Generalized Alignment Index (GALI)

SALI effectively measures the ‘area’ of the parallelogram formed by the two deviation vectors.



Definition of Generalized Alignment Index (GALI)

SALI effectively measures the ‘area’ of the parallelogram formed by the two deviation vectors.



Definition of GALI

In the case of an N degree of freedom Hamiltonian system or a $2N$ symplectic map we follow the evolution of

k deviation vectors with $2 \leq k \leq 2N$,

and define (Ch.S., Bountis, Antonopoulos, 2007, Physica D) the Generalized Alignment Index (GALI) of order k :

$$\text{GALI}_k(t) = \|\hat{\mathbf{v}}_1(t) \wedge \hat{\mathbf{v}}_2(t) \wedge \dots \wedge \hat{\mathbf{v}}_k(t)\|$$

where

$$\hat{\mathbf{v}}_1(t) = \frac{\mathbf{v}_1(t)}{\|\mathbf{v}_1(t)\|}$$

Wedge product

We consider as a basis of the $2N$ -dimensional tangent space of the system the usual set of orthonormal vectors:

$$\hat{e}_1 = (1, 0, 0, \dots, 0), \hat{e}_2 = (0, 1, 0, \dots, 0), \dots, \hat{e}_{2N} = (0, 0, 0, \dots, 1)$$

Then for k deviation vectors we have:

$$\begin{bmatrix} \hat{v}_1 \\ \hat{v}_2 \\ \vdots \\ \hat{v}_k \end{bmatrix} = \begin{bmatrix} v_{11} & v_{12} & \cdots & v_{12N} \\ v_{21} & v_{22} & \cdots & v_{22N} \\ \vdots & \vdots & & \vdots \\ v_{k1} & v_{k2} & \cdots & v_{k2N} \end{bmatrix} \cdot \begin{bmatrix} \hat{e}_1 \\ \hat{e}_2 \\ \vdots \\ \hat{e}_{2N} \end{bmatrix}$$

$$\hat{v}_1 \wedge \hat{v}_2 \wedge \cdots \wedge \hat{v}_k = \sum_{1 \leq i_1 < i_2 < \cdots < i_k \leq 2N} \begin{vmatrix} v_{1i_1} & v_{1i_2} & \cdots & v_{1i_k} \\ v_{2i_1} & v_{2i_2} & \cdots & v_{2i_k} \\ \vdots & \vdots & & \vdots \\ v_{ki_1} & v_{ki_2} & \cdots & v_{ki_k} \end{vmatrix} \hat{e}_{i_1} \wedge \hat{e}_{i_2} \wedge \cdots \wedge \hat{e}_{i_k}$$

Norm of wedge product

We define as ‘**norm**’ of the wedge product the quantity :

$$\|\hat{\mathbf{v}}_1 \wedge \hat{\mathbf{v}}_2 \wedge \cdots \wedge \hat{\mathbf{v}}_k\| = \left\{ \sum_{1 \leq i_1 < i_2 < \cdots < i_k \leq 2N} \left| \begin{array}{cccc} \mathbf{v}_{1 i_1} & \mathbf{v}_{1 i_2} & \cdots & \mathbf{v}_{1 i_k} \\ \mathbf{v}_{2 i_1} & \mathbf{v}_{2 i_2} & \cdots & \mathbf{v}_{2 i_k} \\ \vdots & \vdots & & \vdots \\ \mathbf{v}_{k i_1} & \mathbf{v}_{k i_2} & \cdots & \mathbf{v}_{k i_k} \end{array} \right|^2 \right\}^{1/2}$$

Computation of GALI - Example

Let us compute GALI_3 in the case of 2D Hamiltonian system (4-dimensional phase space).

$$\begin{bmatrix} \hat{\mathbf{v}}_1 \\ \hat{\mathbf{v}}_2 \\ \hat{\mathbf{v}}_3 \end{bmatrix} = \begin{bmatrix} \mathbf{v}_{11} & \mathbf{v}_{12} & \mathbf{v}_{13} & \mathbf{v}_{14} \\ \mathbf{v}_{21} & \mathbf{v}_{22} & \mathbf{v}_{23} & \mathbf{v}_{24} \\ \mathbf{v}_{31} & \mathbf{v}_{32} & \mathbf{v}_{33} & \mathbf{v}_{34} \end{bmatrix} \cdot \begin{bmatrix} \hat{\mathbf{e}}_1 \\ \hat{\mathbf{e}}_2 \\ \hat{\mathbf{e}}_3 \\ \hat{\mathbf{e}}_4 \end{bmatrix}$$

Computation of GALI - Example

Let us compute GALI_3 in the case of 2D Hamiltonian system (4-dimensional phase space).

$$\begin{bmatrix} \hat{\mathbf{v}}_1 \\ \hat{\mathbf{v}}_2 \\ \hat{\mathbf{v}}_3 \end{bmatrix} = \begin{bmatrix} \mathbf{v}_{11} & \mathbf{v}_{12} & \mathbf{v}_{13} & \mathbf{v}_{14} \\ \mathbf{v}_{21} & \mathbf{v}_{22} & \mathbf{v}_{23} & \mathbf{v}_{24} \\ \mathbf{v}_{31} & \mathbf{v}_{32} & \mathbf{v}_{33} & \mathbf{v}_{34} \end{bmatrix} \cdot \begin{bmatrix} \hat{\mathbf{e}}_1 \\ \hat{\mathbf{e}}_2 \\ \hat{\mathbf{e}}_3 \\ \hat{\mathbf{e}}_4 \end{bmatrix}$$

$$\text{GALI}_3 = \|\hat{\mathbf{v}}_1 \wedge \hat{\mathbf{v}}_2 \wedge \hat{\mathbf{v}}_3\| = \left\{ \begin{array}{c} \text{Columns } \mathbf{1} \quad \mathbf{2} \quad \mathbf{3} \\ \left| \begin{array}{ccc} \mathbf{v}_{11} & \mathbf{v}_{12} & \mathbf{v}_{13} \\ \mathbf{v}_{21} & \mathbf{v}_{22} & \mathbf{v}_{23} \\ \mathbf{v}_{31} & \mathbf{v}_{32} & \mathbf{v}_{33} \end{array} \right|^2 \end{array} \right\} +$$

Computation of GALI - Example

Let us compute GALI_3 in the case of 2D Hamiltonian system (4-dimensional phase space).

$$\begin{bmatrix} \hat{\mathbf{v}}_1 \\ \hat{\mathbf{v}}_2 \\ \hat{\mathbf{v}}_3 \end{bmatrix} = \begin{bmatrix} \mathbf{v}_{11} & \mathbf{v}_{12} & \mathbf{v}_{13} & \mathbf{v}_{14} \\ \mathbf{v}_{21} & \mathbf{v}_{22} & \mathbf{v}_{23} & \mathbf{v}_{24} \\ \mathbf{v}_{31} & \mathbf{v}_{32} & \mathbf{v}_{33} & \mathbf{v}_{34} \end{bmatrix} \cdot \begin{bmatrix} \hat{\mathbf{e}}_1 \\ \hat{\mathbf{e}}_2 \\ \hat{\mathbf{e}}_3 \\ \hat{\mathbf{e}}_4 \end{bmatrix}$$

$$\text{GALI}_3 = \|\hat{\mathbf{v}}_1 \wedge \hat{\mathbf{v}}_2 \wedge \hat{\mathbf{v}}_3\| = \left\{ \begin{array}{c} \text{Columns } \mathbf{1} \quad \mathbf{2} \quad \mathbf{3} \\ \left| \begin{array}{ccc} \mathbf{v}_{11} & \mathbf{v}_{12} & \mathbf{v}_{13} \\ \mathbf{v}_{21} & \mathbf{v}_{22} & \mathbf{v}_{23} \\ \mathbf{v}_{31} & \mathbf{v}_{32} & \mathbf{v}_{33} \end{array} \right|^2 + \left| \begin{array}{ccc} \mathbf{v}_{11} & \mathbf{v}_{12} & \mathbf{v}_{14} \\ \mathbf{v}_{21} & \mathbf{v}_{22} & \mathbf{v}_{24} \\ \mathbf{v}_{31} & \mathbf{v}_{32} & \mathbf{v}_{34} \end{array} \right|^2 + \left| \begin{array}{ccc} \mathbf{v}_{11} & \mathbf{v}_{13} & \mathbf{v}_{14} \\ \mathbf{v}_{21} & \mathbf{v}_{23} & \mathbf{v}_{24} \\ \mathbf{v}_{31} & \mathbf{v}_{33} & \mathbf{v}_{34} \end{array} \right|^2 \end{array} \right\}^{1/2}$$

Computation of GALI - Example

Let us compute GALI_3 in the case of 2D Hamiltonian system (4-dimensional phase space).

$$\begin{bmatrix} \hat{\mathbf{v}}_1 \\ \hat{\mathbf{v}}_2 \\ \hat{\mathbf{v}}_3 \end{bmatrix} = \begin{bmatrix} \mathbf{v}_{11} & \mathbf{v}_{12} & \mathbf{v}_{13} & \mathbf{v}_{14} \\ \mathbf{v}_{21} & \mathbf{v}_{22} & \mathbf{v}_{23} & \mathbf{v}_{24} \\ \mathbf{v}_{31} & \mathbf{v}_{32} & \mathbf{v}_{33} & \mathbf{v}_{34} \end{bmatrix} \cdot \begin{bmatrix} \hat{\mathbf{e}}_1 \\ \hat{\mathbf{e}}_2 \\ \hat{\mathbf{e}}_3 \\ \hat{\mathbf{e}}_4 \end{bmatrix}$$

$$\text{GALI}_3 = \|\hat{\mathbf{v}}_1 \wedge \hat{\mathbf{v}}_2 \wedge \hat{\mathbf{v}}_3\| = \left\{ \begin{array}{c} \text{Columns } \mathbf{1} \quad \mathbf{2} \quad \mathbf{3} \\ \left| \begin{array}{ccc} \mathbf{v}_{11} & \mathbf{v}_{12} & \mathbf{v}_{13} \\ \mathbf{v}_{21} & \mathbf{v}_{22} & \mathbf{v}_{23} \\ \mathbf{v}_{31} & \mathbf{v}_{32} & \mathbf{v}_{33} \end{array} \right|^2 + \left| \begin{array}{ccc} \mathbf{v}_{11} & \mathbf{v}_{12} & \mathbf{v}_{14} \\ \mathbf{v}_{21} & \mathbf{v}_{22} & \mathbf{v}_{24} \\ \mathbf{v}_{31} & \mathbf{v}_{32} & \mathbf{v}_{34} \end{array} \right|^2 + \\ \left| \begin{array}{ccc} \mathbf{v}_{11} & \mathbf{v}_{13} & \mathbf{v}_{14} \\ \mathbf{v}_{21} & \mathbf{v}_{23} & \mathbf{v}_{24} \\ \mathbf{v}_{31} & \mathbf{v}_{33} & \mathbf{v}_{34} \end{array} \right|^2 \end{array} \right\} +$$

$\mathbf{1} \quad \mathbf{3} \quad \mathbf{4}$

Computation of GALI - Example

Let us compute GALI_3 in the case of 2D Hamiltonian system (4-dimensional phase space).

$$\begin{bmatrix} \hat{\mathbf{v}}_1 \\ \hat{\mathbf{v}}_2 \\ \hat{\mathbf{v}}_3 \end{bmatrix} = \begin{bmatrix} \mathbf{v}_{11} & \mathbf{v}_{12} & \mathbf{v}_{13} & \mathbf{v}_{14} \\ \mathbf{v}_{21} & \mathbf{v}_{22} & \mathbf{v}_{23} & \mathbf{v}_{24} \\ \mathbf{v}_{31} & \mathbf{v}_{32} & \mathbf{v}_{33} & \mathbf{v}_{34} \end{bmatrix} \cdot \begin{bmatrix} \hat{\mathbf{e}}_1 \\ \hat{\mathbf{e}}_2 \\ \hat{\mathbf{e}}_3 \\ \hat{\mathbf{e}}_4 \end{bmatrix}$$

$$\text{GALI}_3 = \|\hat{\mathbf{v}}_1 \wedge \hat{\mathbf{v}}_2 \wedge \hat{\mathbf{v}}_3\| = \left\{ \begin{array}{c} \text{Columns } \mathbf{1} \quad \mathbf{2} \quad \mathbf{3} \\ \left| \begin{array}{ccc} \mathbf{v}_{11} & \mathbf{v}_{12} & \mathbf{v}_{13} \\ \mathbf{v}_{21} & \mathbf{v}_{22} & \mathbf{v}_{23} \\ \mathbf{v}_{31} & \mathbf{v}_{32} & \mathbf{v}_{33} \end{array} \right|^2 + \left| \begin{array}{ccc} \mathbf{v}_{11} & \mathbf{v}_{12} & \mathbf{v}_{14} \\ \mathbf{v}_{21} & \mathbf{v}_{22} & \mathbf{v}_{24} \\ \mathbf{v}_{31} & \mathbf{v}_{32} & \mathbf{v}_{34} \end{array} \right|^2 + \\ \left| \begin{array}{ccc} \mathbf{v}_{11} & \mathbf{v}_{13} & \mathbf{v}_{14} \\ \mathbf{v}_{21} & \mathbf{v}_{23} & \mathbf{v}_{24} \\ \mathbf{v}_{31} & \mathbf{v}_{33} & \mathbf{v}_{34} \end{array} \right|^2 + \left| \begin{array}{ccc} \mathbf{v}_{12} & \mathbf{v}_{13} & \mathbf{v}_{14} \\ \mathbf{v}_{22} & \mathbf{v}_{23} & \mathbf{v}_{24} \\ \mathbf{v}_{32} & \mathbf{v}_{33} & \mathbf{v}_{34} \end{array} \right|^2 \end{array} \right\}^{1/2}$$

$\mathbf{1} \quad \mathbf{3} \quad \mathbf{4} \quad \mathbf{2} \quad \mathbf{3} \quad \mathbf{4}$

Efficient computation of GALI

For k deviation vectors:

$$\begin{bmatrix} \hat{\mathbf{v}}_1 \\ \hat{\mathbf{v}}_2 \\ \vdots \\ \hat{\mathbf{v}}_k \end{bmatrix} = \begin{bmatrix} \mathbf{v}_{11} & \mathbf{v}_{12} & \cdots & \mathbf{v}_{12N} \\ \mathbf{v}_{21} & \mathbf{v}_{22} & \cdots & \mathbf{v}_{22N} \\ \vdots & \vdots & & \vdots \\ \mathbf{v}_{k1} & \mathbf{v}_{k2} & \cdots & \mathbf{v}_{k2N} \end{bmatrix} \cdot \begin{bmatrix} \hat{\mathbf{e}}_1 \\ \hat{\mathbf{e}}_2 \\ \vdots \\ \hat{\mathbf{e}}_{2N} \end{bmatrix} = \mathbf{A} \cdot \begin{bmatrix} \hat{\mathbf{e}}_1 \\ \hat{\mathbf{e}}_2 \\ \vdots \\ \hat{\mathbf{e}}_{2N} \end{bmatrix}$$

the ‘norm’ of the wedge product is given by:

$$\|\hat{\mathbf{v}}_1 \wedge \hat{\mathbf{v}}_2 \wedge \cdots \wedge \hat{\mathbf{v}}_k\| = \left\{ \sum_{1 \leq i_1 < i_2 < \cdots < i_k \leq 2N} \left| \begin{array}{cccc} \mathbf{v}_{1i_1} & \mathbf{v}_{1i_2} & \cdots & \mathbf{v}_{1i_k} \\ \mathbf{v}_{2i_1} & \mathbf{v}_{2i_2} & \cdots & \mathbf{v}_{2i_k} \\ \vdots & \vdots & & \vdots \\ \mathbf{v}_{ki_1} & \mathbf{v}_{ki_2} & \cdots & \mathbf{v}_{ki_k} \end{array} \right|^2 \right\}^{1/2} = \sqrt{\det(\mathbf{A} \cdot \mathbf{A}^T)}$$

Efficient computation of GALI

From **Singular Value Decomposition (SVD)** of A^T we get:

$$A^T = U \cdot W \cdot V^T$$

where U is a column-orthogonal $2N \times k$ matrix ($U^T \cdot U = I$), V^T is a $k \times k$ orthogonal matrix ($V \cdot V^T = I$), and W is a diagonal $k \times k$ matrix with positive or zero elements, the so-called **singular values**. So, we get:

$$\begin{aligned} \det(A \cdot A^T) &= \det(V \cdot W^T \cdot U^T \cdot U \cdot W \cdot V^T) = \det(V \cdot W \cdot I \cdot W \cdot V^T) = \\ \det(V \cdot W^2 \cdot V^T) &= \det(V \cdot \text{diag}(w_1^2, w_2^2, \dots, w_k^2) \cdot V^T) = \prod_{i=1}^k w_i^2 \end{aligned}$$

Thus, GALI_k is computed by:

$$\text{GALI}_k = \sqrt{\det(A \cdot A^T)} = \prod_{i=1}^k w_i \Rightarrow \log(\text{GALI}_k) = \sum_{i=1}^k \log(w_i)$$

Behavior of $GALI_k$ for chaotic motion

$GALI_k$ ($2 \leq k \leq 2N$) tends exponentially to zero with exponents that involve the values of the first k largest Lyapunov exponents $\sigma_1, \sigma_2, \dots, \sigma_k$:

$$GALI_k(t) \propto e^{-[(\sigma_1 - \sigma_2) + (\sigma_1 - \sigma_3) + \dots + (\sigma_1 - \sigma_k)]t}$$

The above relation is valid even if some Lyapunov exponents are equal, or very close to each other.

Behavior of $GALI_k$ for chaotic motion

Using the approximation:

$$\mathbf{v}_i(t) = \sum_{j=1}^{2N} \mathbf{c}_j^i e^{\sigma_j t} \hat{\mathbf{u}}_j = \mathbf{c}_1^i e^{\sigma_1 t} \hat{\mathbf{u}}_1 + \mathbf{c}_2^i e^{\sigma_2 t} \hat{\mathbf{u}}_2 + \dots + \mathbf{c}_{2N}^i e^{\sigma_{2N} t} \hat{\mathbf{u}}_{2N}, \quad \|\mathbf{v}_i(t)\| \approx |\mathbf{c}_1^i| e^{\sigma_1 t}$$

where $\sigma_1 > \sigma_2 \geq \dots \geq \sigma_n$ are the **Lyapunov exponents**, and $\hat{\mathbf{u}}_j$ $j=1, 2, \dots, 2N$ the corresponding eigendirections, we get

$$\begin{bmatrix} \hat{\mathbf{v}}_1 \\ \hat{\mathbf{v}}_2 \\ \vdots \\ \hat{\mathbf{v}}_k \end{bmatrix} = \begin{bmatrix} s_1 & \frac{\mathbf{c}_2^1}{|\mathbf{c}_1^1|} e^{-(\sigma_1 - \sigma_2)t} & \frac{\mathbf{c}_3^1}{|\mathbf{c}_1^1|} e^{-(\sigma_1 - \sigma_3)t} & \dots & \frac{\mathbf{c}_{2N}^1}{|\mathbf{c}_1^1|} e^{-(\sigma_1 - \sigma_{2N})t} \\ s_2 & \frac{\mathbf{c}_2^2}{|\mathbf{c}_1^2|} e^{-(\sigma_1 - \sigma_2)t} & \frac{\mathbf{c}_3^2}{|\mathbf{c}_1^2|} e^{-(\sigma_1 - \sigma_3)t} & \dots & \frac{\mathbf{c}_{2N}^2}{|\mathbf{c}_1^2|} e^{-(\sigma_1 - \sigma_{2N})t} \\ \vdots & \vdots & \vdots & \vdots & \vdots \\ s_k & \frac{\mathbf{c}_2^k}{|\mathbf{c}_1^k|} e^{-(\sigma_1 - \sigma_2)t} & \frac{\mathbf{c}_3^k}{|\mathbf{c}_1^k|} e^{-(\sigma_1 - \sigma_3)t} & \dots & \frac{\mathbf{c}_{2N}^k}{|\mathbf{c}_1^k|} e^{-(\sigma_1 - \sigma_{2N})t} \end{bmatrix} \cdot \begin{bmatrix} \hat{\mathbf{u}}_1 \\ \hat{\mathbf{u}}_2 \\ \vdots \\ \hat{\mathbf{u}}_{2N} \end{bmatrix}$$

with $s_i = \text{sign}(\mathbf{c}_1^i)$.

Behavior of $GALI_k$ for chaotic motion

From all determinants appearing in the definition of $GALI_k$ the one that **decreases the slowest** is the one containing the first k columns of the previous matrix:

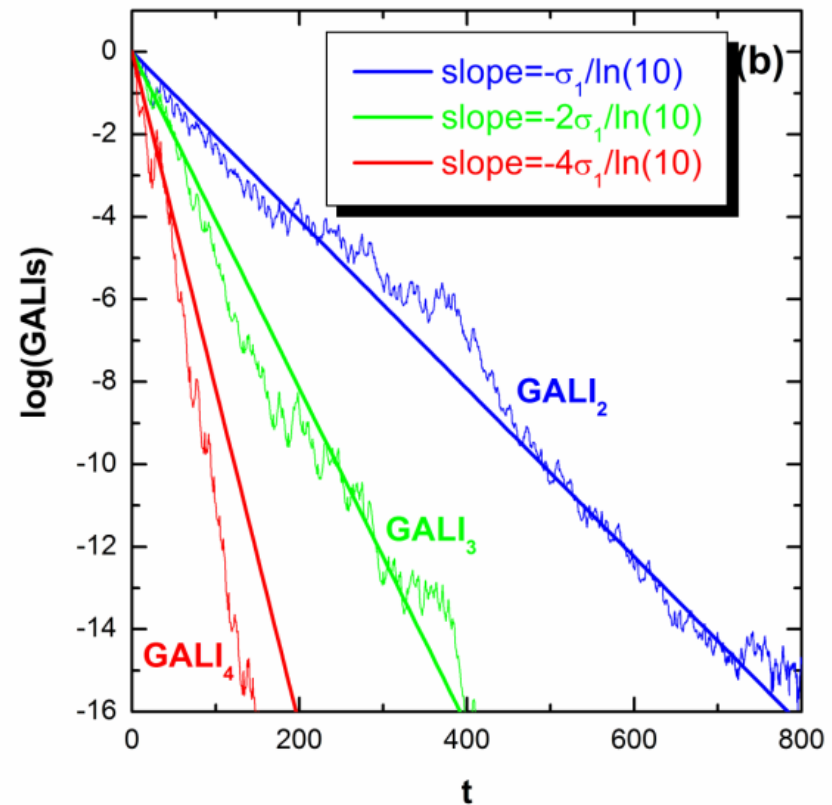
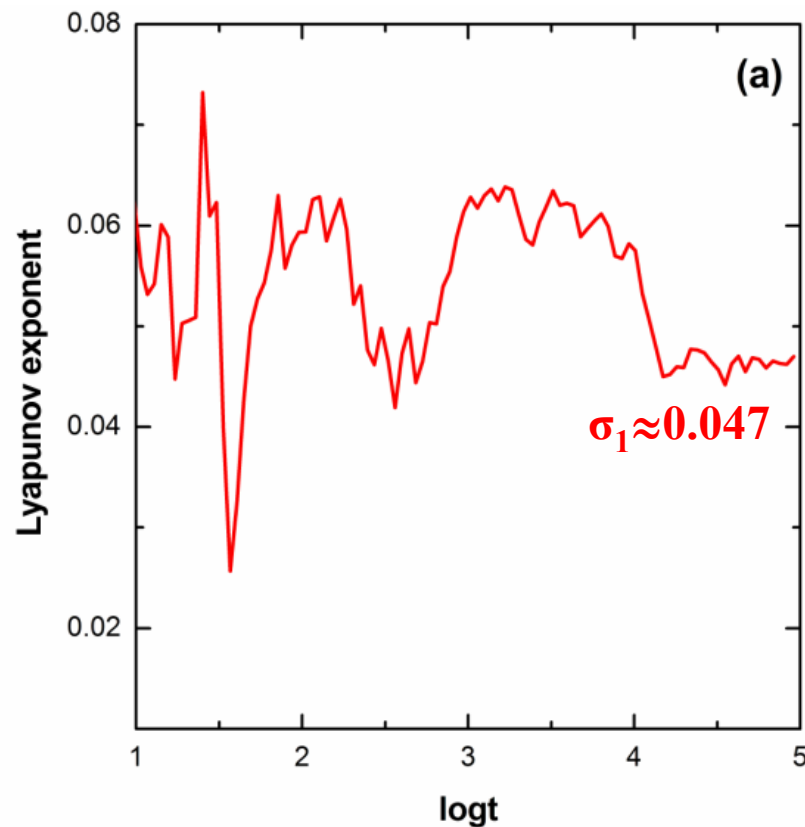
$$\begin{vmatrix} s_1 & \frac{c_2^1}{|c_1^1|} e^{-(\sigma_1 - \sigma_2)t} & \frac{c_3^1}{|c_1^1|} e^{-(\sigma_1 - \sigma_3)t} & \dots & \frac{c_k^1}{|c_1^1|} e^{-(\sigma_1 - \sigma_k)t} \\ s_2 & \frac{c_2^2}{|c_1^2|} e^{-(\sigma_1 - \sigma_2)t} & \frac{c_3^2}{|c_1^2|} e^{-(\sigma_1 - \sigma_3)t} & \dots & \frac{c_k^2}{|c_1^2|} e^{-(\sigma_1 - \sigma_k)t} \\ \vdots & \vdots & \vdots & \vdots & \vdots \\ s_k & \frac{c_2^k}{|c_1^k|} e^{-(\sigma_1 - \sigma_2)t} & \frac{c_3^k}{|c_1^k|} e^{-(\sigma_1 - \sigma_3)t} & \dots & \frac{c_k^k}{|c_1^k|} e^{-(\sigma_1 - \sigma_k)t} \end{vmatrix} = \begin{vmatrix} s_1 & \frac{c_2^1}{|c_1^1|} & \frac{c_3^1}{|c_1^1|} & \dots & \frac{c_k^1}{|c_1^1|} \\ s_2 & \frac{c_2^2}{|c_1^2|} & \frac{c_3^2}{|c_1^2|} & \dots & \frac{c_k^2}{|c_1^2|} \\ \vdots & \vdots & \vdots & \vdots & \vdots \\ s_k & \frac{c_2^k}{|c_1^k|} & \frac{c_3^k}{|c_1^k|} & \dots & \frac{c_k^k}{|c_1^k|} \end{vmatrix} \cdot e^{-[(\sigma_1 - \sigma_2) + (\sigma_1 - \sigma_3) + \dots + (\sigma_1 - \sigma_k)]t}$$

Thus

$$GALI_k(t) \propto e^{-[(\sigma_1 - \sigma_2) + (\sigma_1 - \sigma_3) + \dots + (\sigma_1 - \sigma_k)]t}$$

Behavior of $GALI_k$ for chaotic motion

2D Hamiltonian (Hénon-Heiles system)

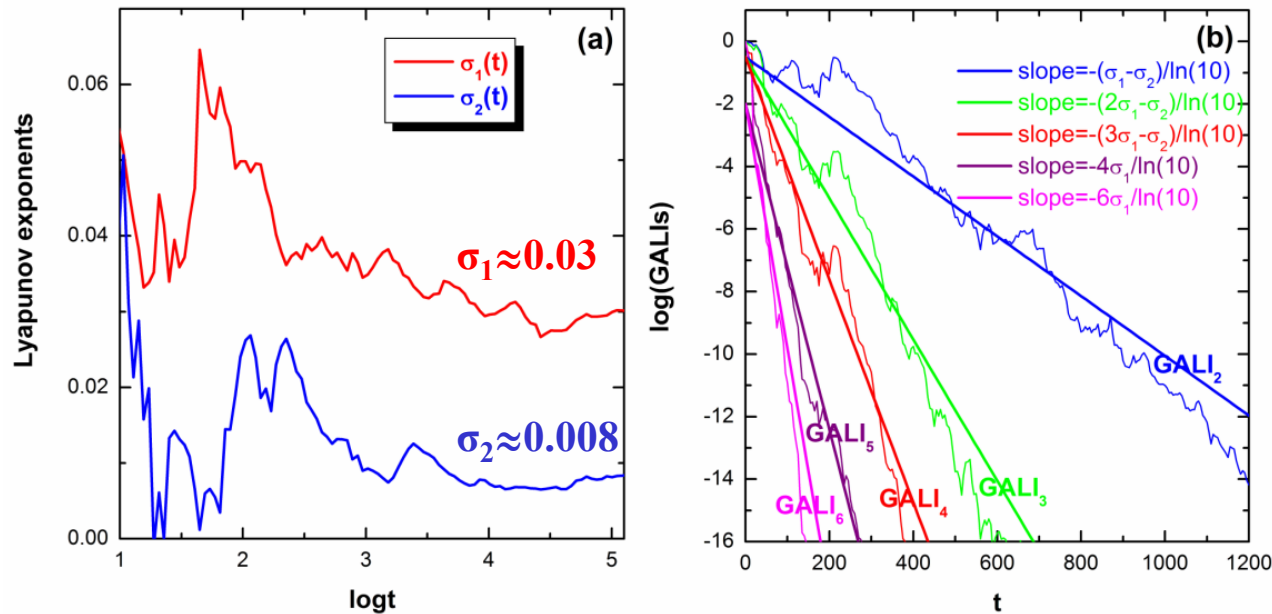


Behavior of $GALI_k$ for chaotic motion

3D system:

$$H_3 = \sum_{i=1}^3 \frac{\omega_i}{2} (q_i^2 + p_i^2) + q_1^2 q_2 + q_1^2 q_3$$

with $\omega_1=1$, $\omega_2=\sqrt{2}$, $\omega_3=\sqrt{3}$, $H_3=0.09$.

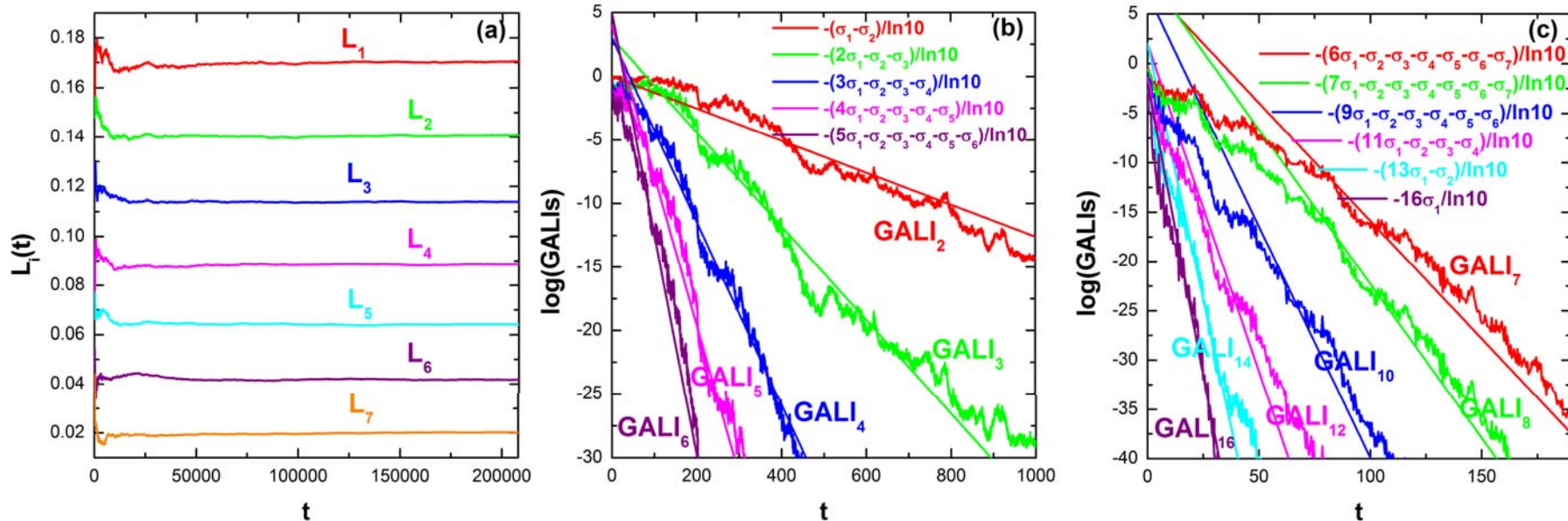


Behavior of GALI_k for chaotic motion

N particles Fermi-Pasta-Ulam (FPU) system:

$$H = \frac{1}{2} \sum_{i=1}^N p_i^2 + \sum_{i=0}^N \left[\frac{1}{2} (q_{i+1} - q_i)^2 + \frac{\beta}{4} (q_{i+1} - q_i)^4 \right]$$

with fixed boundary conditions, $N=8$ and $\beta=1.5$.



Behavior of GALI_k for regular motion

If the motion occurs on an **s-dimensional torus** with **$s \leq N$** then the behavior of GALI_k is given by (Ch.S., Bountis, Antonopoulos, 2008, Eur. Phys. J. Sp. Top.):

$$\text{GALI}_k(t) \propto \begin{cases} \text{constant} & \text{if } 2 \leq k \leq s \\ \frac{1}{t^{k-s}} & \text{if } s < k \leq 2N - s \\ \frac{1}{t^{2(k-N)}} & \text{if } 2N - s < k \leq 2N \end{cases}$$

while in the **common case with $s=N$** we have :

$$\text{GALI}_k(t) \propto \begin{cases} \text{constant} & \text{if } 2 \leq k \leq N \\ \frac{1}{t^{2(k-N)}} & \text{if } N < k \leq 2N \end{cases}$$

Behavior of $GALI_k$ for regular motion

Regular orbits of an N degree of freedom Hamiltonian system lie on **N -dimensional tori**.

Performing a **local transformation to action-angle variables** we get for the Hamilton's equations of motion:

$$\left. \begin{array}{l} \dot{J}_i = 0 \\ \dot{\theta}_i = \omega_i(J_1, J_2, \dots, J_N) \end{array} \right\} \Rightarrow \left. \begin{array}{l} J_i(t) = J_{i0} \\ \theta_i(t) = \theta_{i0} + \omega_i(J_{10}, J_{20}, \dots, J_{N0}) \cdot t \end{array} \right\}, \quad i = 1, 2, \dots, N$$

where $J_{i0}, \theta_{i0}, i=1, 2, \dots, N$ are the initial conditions.

Behavior of GALI_k for regular motion

The variational equations give:

$$\left. \begin{aligned} \dot{\xi}_i &= 0 \\ \dot{\eta}_i &= \sum_{j=1}^N \omega_{ij} \cdot \xi_j \end{aligned} \right\} \Rightarrow \begin{aligned} \xi_i(t) &= \xi_i(0) \\ \eta_i(t) &= \eta_i(0) + \left[\sum_{j=1}^N \omega_{ij} \cdot \xi_j(0) \right] \cdot t, \quad i = 1, 2, \dots, N \end{aligned}$$

where $\omega_{ij} = \partial \omega_i / \partial J_j|_{J_0}$, $i=1, 2, \dots, N$ are constants.

Using as a basis of the $2N$ -dimensional tangent space of the flow the $2N$ unit vectors $\{\hat{u}_1, \hat{u}_2, \dots, \hat{u}_{2N}\}$ such that the first N of them, $\hat{u}_1, \hat{u}_2, \dots, \hat{u}_N$ correspond to the N action variables and the N remaining ones, $\hat{u}_{N+1}, \hat{u}_{N+2}, \dots, \hat{u}_{2N}$ to the conjugate angle variables, we write any unit deviation vector as:

$$\hat{v}_i(t) = \frac{1}{\|\mathbf{v}_i(t)\|} \left[\sum_{j=1}^N \xi_j^i(0) \hat{u}_j + \sum_{j=1}^N \left(\eta_j^i(0) + \sum_{k=1}^N \omega_{kj} \xi_j^i(0) t \right) \hat{u}_{N+j} \right]$$

with $\|\mathbf{v}_i(t)\| \propto t$

Behavior of GALI_k for regular motion

For k deviation vectors we have:

$$\begin{bmatrix} \hat{\mathbf{v}}_1 \\ \hat{\mathbf{v}}_2 \\ \vdots \\ \hat{\mathbf{v}}_k \end{bmatrix} = \frac{1}{\prod_{m=1}^k \|\mathbf{v}_m(t)\|} \cdot \begin{bmatrix} \xi_1^1(0) & \dots & \xi_N^1(0) & \eta_1^1(0) + \sum_{m=1}^N \omega_{1m} \xi_m^1(0) t & \dots & \eta_N^1(0) + \sum_{m=1}^N \omega_{Nm} \xi_m^1(0) t \\ \xi_1^2(0) & \dots & \xi_N^2(0) & \eta_1^2(0) + \sum_{m=1}^N \omega_{1m} \xi_m^2(0) t & \dots & \eta_N^2(0) + \sum_{m=1}^N \omega_{Nm} \xi_m^2(0) t \\ \vdots & & \vdots & \vdots & & \vdots \\ \xi_1^k(0) & \dots & \xi_N^k(0) & \eta_1^k(0) + \sum_{m=1}^N \omega_{1m} \xi_m^k(0) t & \dots & \eta_N^k(0) + \sum_{m=1}^N \omega_{Nm} \xi_m^k(0) t \end{bmatrix} \cdot \begin{bmatrix} \hat{\mathbf{u}}_1 \\ \hat{\mathbf{u}}_2 \\ \vdots \\ \hat{\mathbf{u}}_{2N} \end{bmatrix}$$

Behavior of $GALI_k$ for regular motion

For $2 \leq k \leq N$ the slowest decreasing determinants are the ones whose k columns are chosen among the last N columns of the evolution matrix

$$\frac{1}{\prod_{m=1}^k \|v_m(t)\|} \cdot \begin{vmatrix} \eta_{j_1}^1(0) + \sum_{m=1}^N \omega_{j_1 m} \xi_m^1(0) t & \dots & \eta_{j_k}^1(0) + \sum_{m=1}^N \omega_{j_k m} \xi_m^1(0) t \\ \eta_{j_1}^2(0) + \sum_{m=1}^N \omega_{j_1 m} \xi_m^2(0) t & \dots & \eta_{j_k}^2(0) + \sum_{m=1}^N \omega_{j_k m} \xi_m^2(0) t \\ \vdots & & \vdots \\ \eta_{j_1}^k(0) + \sum_{m=1}^N \omega_{j_1 m} \xi_m^k(0) t & \dots & \eta_{j_k}^k(0) + \sum_{m=1}^N \omega_{j_k m} \xi_m^k(0) t \end{vmatrix} \propto$$

$$\propto \frac{1}{t^k} \cdot \begin{vmatrix} \omega_{j_1 m_1} \xi_{m_1}^1(0) t & \dots & \omega_{j_k m_k} \xi_{m_k}^1(0) t \\ \omega_{j_1 m_1} \xi_{m_1}^2(0) t & \dots & \omega_{j_k m_k} \xi_{m_k}^2(0) t \\ \vdots & & \vdots \\ \omega_{j_1 m_1} \xi_{m_1}^k(0) t & \dots & \omega_{j_k m_k} \xi_{m_k}^k(0) t \end{vmatrix} \propto \frac{1}{t^k} \cdot t^k \cdot \begin{vmatrix} \omega_{j_1 m_1} \xi_{m_1}^1(0) & \dots & \omega_{j_k m_k} \xi_{m_k}^1(0) \\ \omega_{j_1 m_1} \xi_{m_1}^2(0) & \dots & \omega_{j_k m_k} \xi_{m_k}^2(0) \\ \vdots & & \vdots \\ \omega_{j_1 m_1} \xi_{m_1}^k(0) & \dots & \omega_{j_k m_k} \xi_{m_k}^k(0) \end{vmatrix} \approx \text{constant}$$

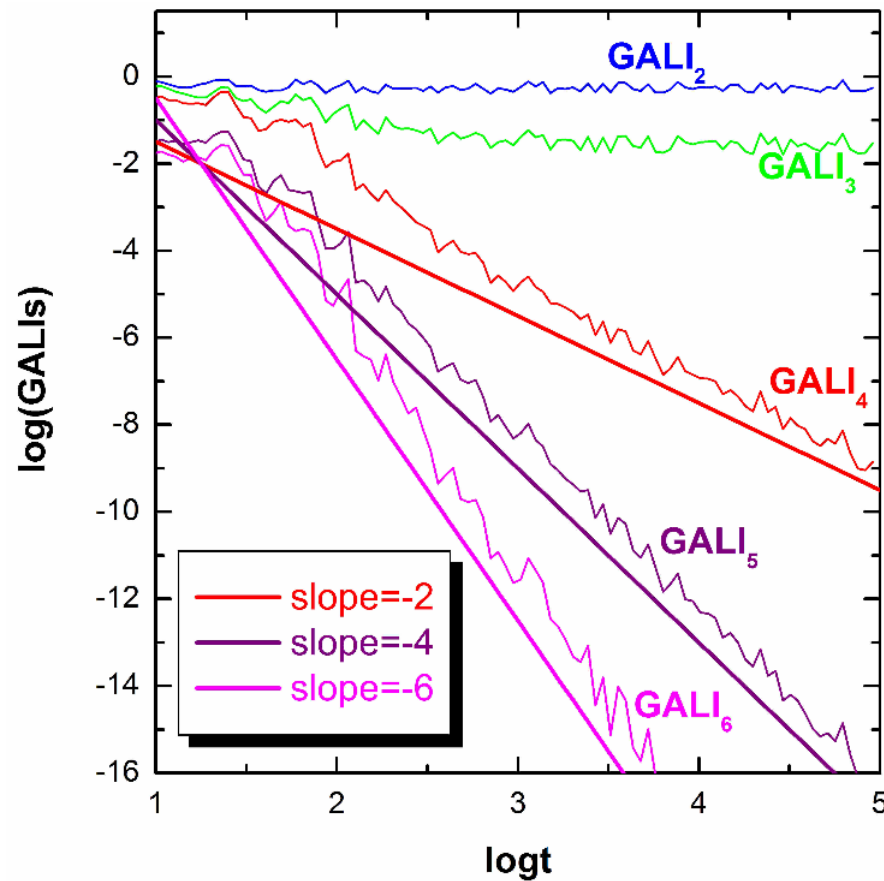
Behavior of GALI_k for regular motion

For $N < k \leq 2N$ the slowest decreasing determinants are the ones containing the last N columns of the evolution matrix

$$\begin{aligned}
 & \frac{1}{\prod_{m=1}^k \|v_m(t)\|} \cdot \begin{vmatrix} \xi_{j_1}^1(0) & \dots & \xi_{j_{k-N}}^1(0) & \eta_1^1(0) + \sum_{m=1}^N \omega_{1m} \xi_m^1(0) t & \dots & \eta_N^1(0) + \sum_{m=1}^N \omega_{Nm} \xi_m^1(0) t \\ \xi_{j_1}^2(0) & \dots & \xi_{j_{k-N}}^2(0) & \eta_1^2(0) + \sum_{m=1}^N \omega_{1m} \xi_m^2(0) t & \dots & \eta_N^2(0) + \sum_{m=1}^N \omega_{Nm} \xi_m^2(0) t \\ \vdots & & \vdots & \vdots & & \vdots \\ \xi_{j_1}^k(0) & \dots & \xi_{j_{k-N}}^k(0) & \eta_1^k(0) + \sum_{m=1}^N \omega_{1m} \xi_m^k(0) t & \dots & \eta_N^k(0) + \sum_{m=1}^N \omega_{Nm} \xi_m^k(0) t \end{vmatrix} \propto \\
 & \begin{matrix} \text{k-N columns} & \text{k-N columns} & \text{2N-k columns} \end{matrix} \\
 & \propto \frac{1}{t^k} \cdot \begin{vmatrix} \xi_{j_1}^1(0) & \dots & \xi_{j_{k-N}}^1(0) & \eta_{i_1}^1(0) & \dots & \eta_{i_{k-N}}^1(0) & \omega_{i_{k-N+1}m_1} \xi_{m_1}^1(0) t & \dots & \omega_{i_N m_{2N-k}} \xi_{m_1}^1(0) t \\ \xi_{j_1}^2(0) & \dots & \xi_{j_{k-N}}^2(0) & \eta_{i_1}^2(0) & \dots & \eta_{i_{k-N}}^2(0) & \omega_{i_{k-N+1}m_1} \xi_{m_1}^2(0) t & \dots & \omega_{i_N m_{2N-k}} \xi_{m_1}^2(0) t \\ \vdots & & \vdots & \vdots & & \vdots & \vdots & & \vdots \\ \xi_{j_1}^k(0) & \dots & \xi_{j_{k-N}}^k(0) & \eta_{i_1}^k(0) & \dots & \eta_{i_{k-N}}^k(0) & \omega_{i_{k-N+1}m_1} \xi_{m_1}^k(0) t & \dots & \omega_{i_N m_{2N-k}} \xi_{m_1}^k(0) t \end{vmatrix} \propto \frac{1}{t^k} \cdot t^{2N-k} \approx \frac{1}{t^{2(k-N)}}
 \end{aligned}$$

Behavior of GALI_k for regular motion

3D Hamiltonian



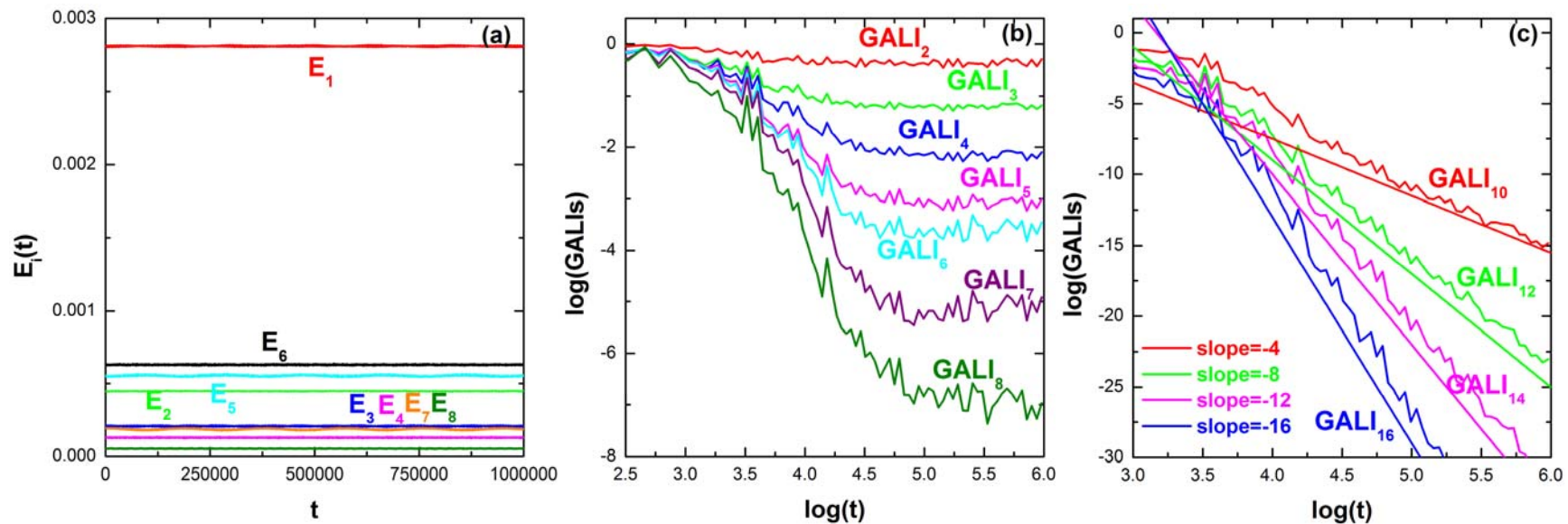
Behavior of GALI_k for regular motion

N=8 FPU system: The unperturbed Hamiltonian ($\beta=0$) is written as a sum of the so-called **harmonic energies** E_i :

$$E_i = \frac{1}{2} (P_i^2 + \omega_i^2 Q_i^2), \quad i = 1, \dots, N$$

with:

$$Q_i = \sqrt{\frac{2}{N+1}} \sum_{i=1}^N q_i \sin\left(\frac{ki\pi}{N+1}\right), \quad P_i = \sqrt{\frac{2}{N+1}} \sum_{i=1}^N p_i \sin\left(\frac{ki\pi}{N+1}\right), \quad \omega_i = 2 \sin\left(\frac{i\pi}{2(N+1)}\right)$$



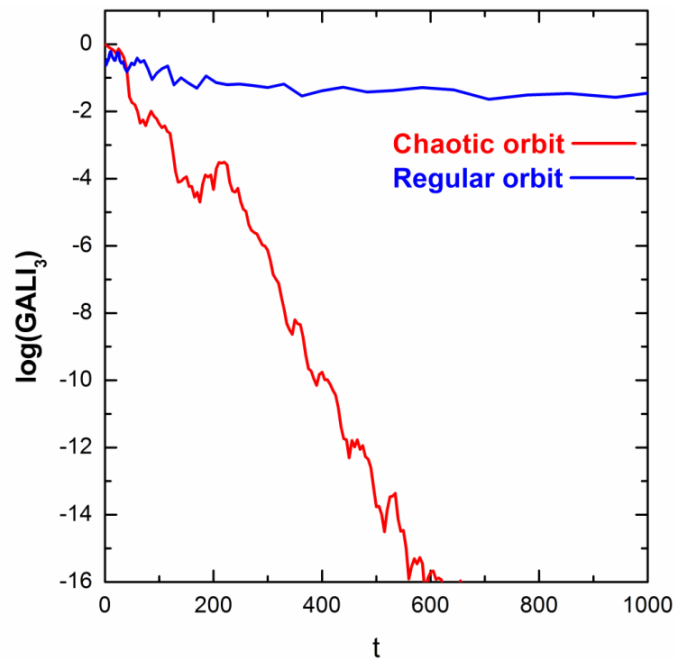
Global dynamics

- $GALI_2$ (practically equivalent to the use of SALI)

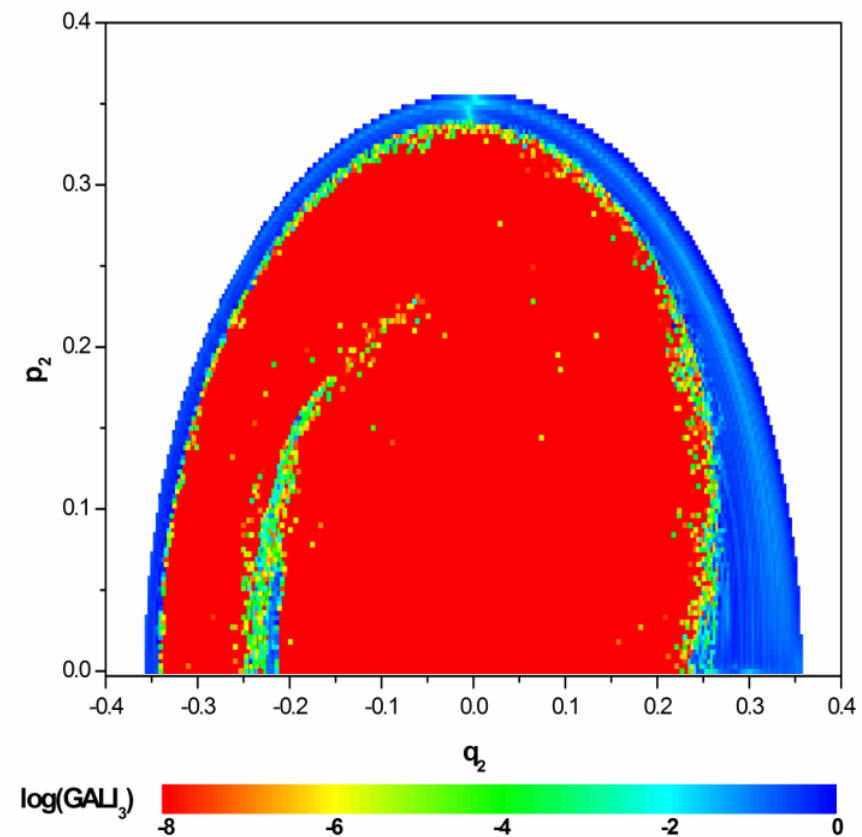
- $GALI_N$

Chaotic motion: $GALI_N \rightarrow 0$
(exponential decay)

Regular motion:
 $GALI_N \rightarrow \text{constant} \neq 0$



3D Hamiltonian
Subspace $q_3=p_3=0$, $p_2 \geq 0$ for $t=1000$.



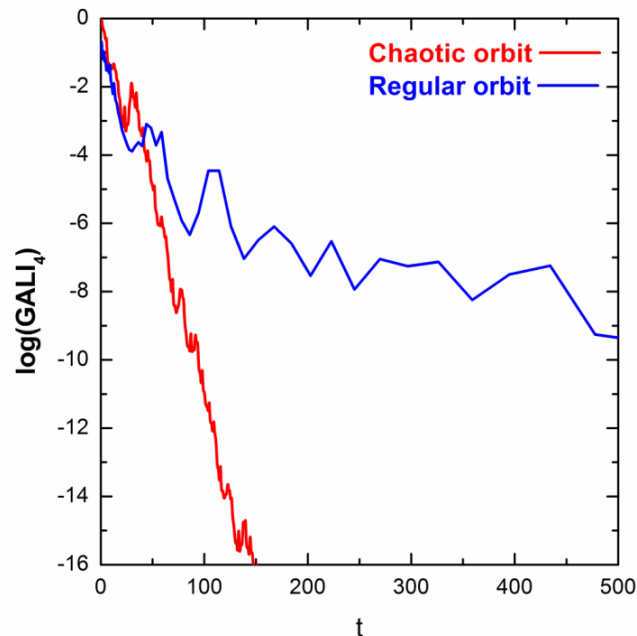
Global dynamics

$GALI_k$ with $k > N$

The index tends to zero both for regular and chaotic orbits but with completely different time rates:

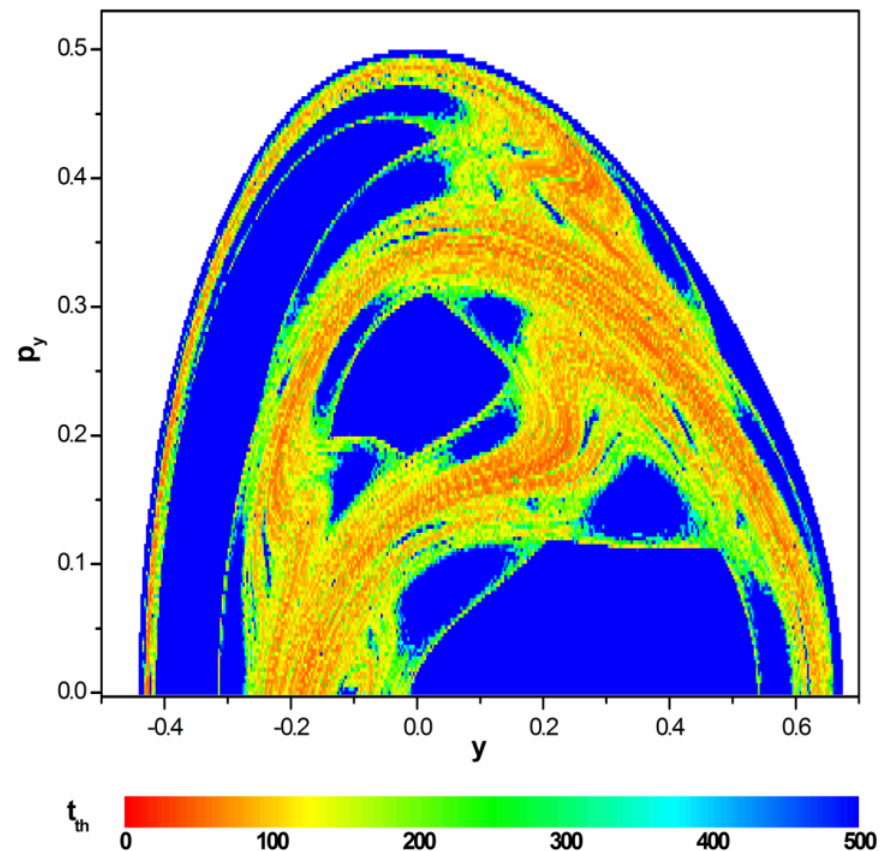
Chaotic motion: exponential decay

Regular motion: power law



2D Hamiltonian (Hénon-Heiles)

Time needed for $GALI_4 < 10^{-12}$



Behavior of $GALI_k$

Chaotic motion:

$GALI_k \rightarrow 0$ exponential decay

$$GALI_k(t) \propto e^{-[(\sigma_1 - \sigma_2) + (\sigma_1 - \sigma_3) + \dots + (\sigma_1 - \sigma_k)]t}$$

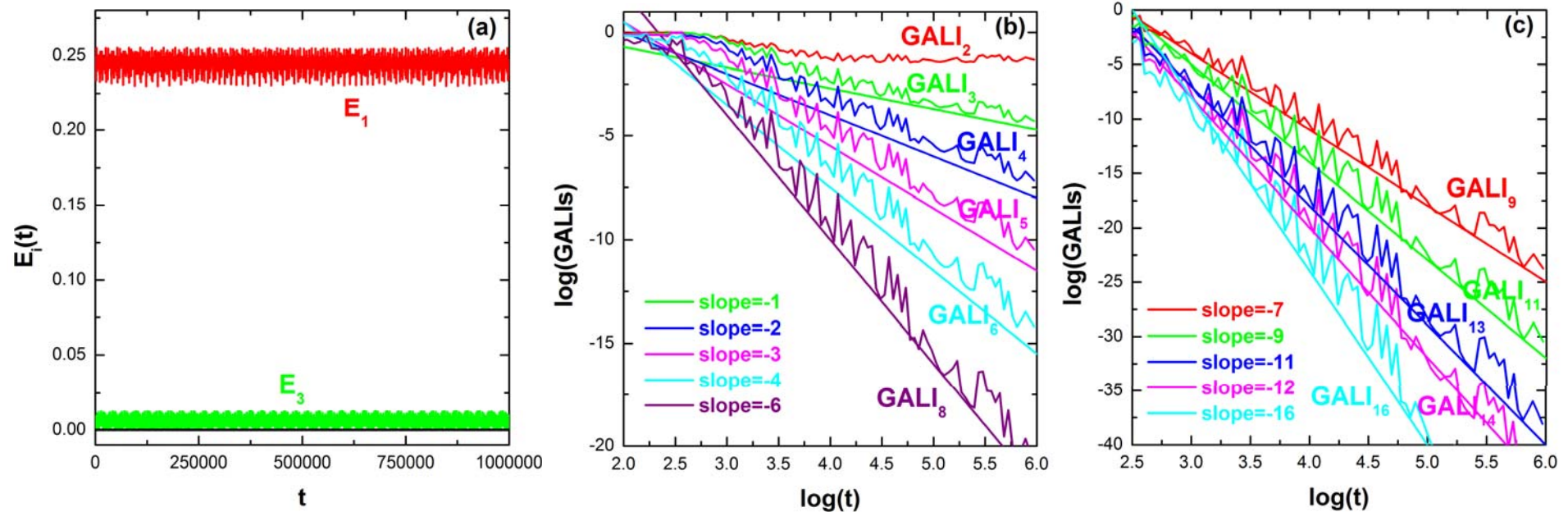
Regular motion:

$GALI_k \rightarrow \text{constant} \neq 0$ or $GALI_k \rightarrow 0$ power law decay

$$GALI_k(t) \propto \begin{cases} \text{constant} & \text{if } 2 \leq k \leq s \\ \frac{1}{t^{k-s}} & \text{if } s < k \leq 2N-s \\ \frac{1}{t^{2(k-N)}} & \text{if } 2N-s < k \leq 2N \end{cases}$$

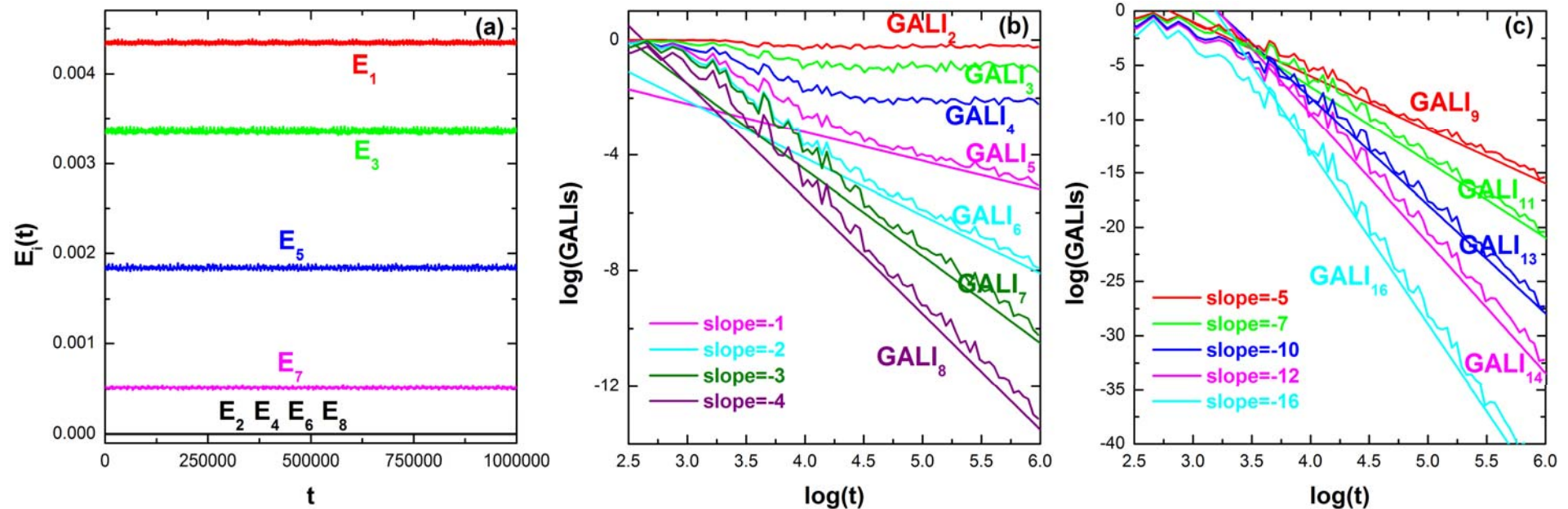
Regular motion on low-dimensional tori

A regular orbit lying on a **2-dimensional torus** for the N=8 FPU system.



Regular motion on low-dimensional tori

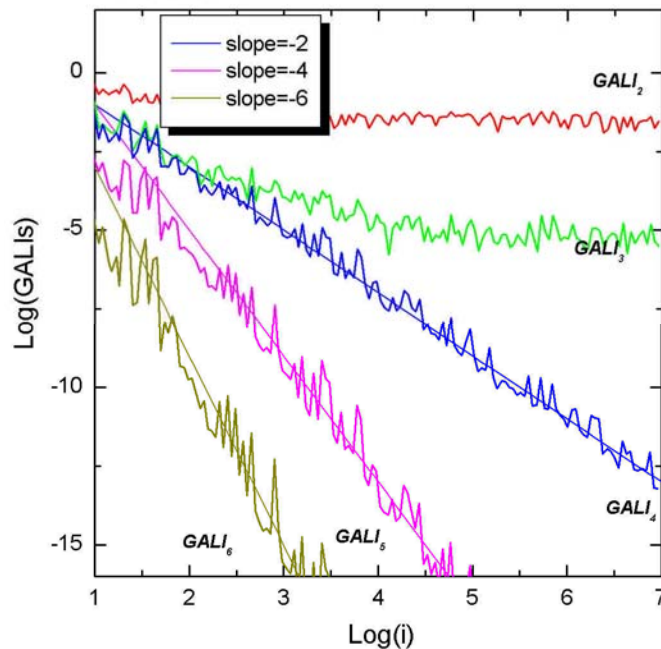
A regular orbit lying on a **4-dimensional torus** for the $N=8$ FPU system.



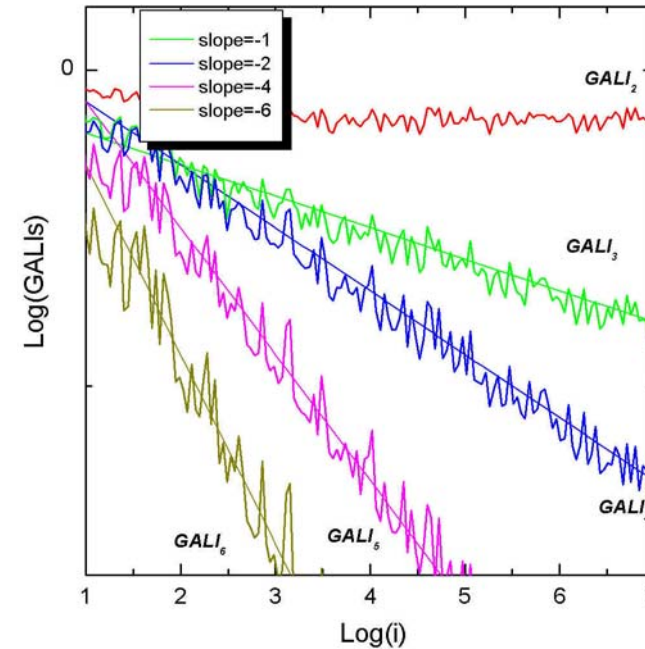
Low-dimensional tori - 6D map

$$\begin{aligned}
 x'_1 &= x_1 + x'_2 \\
 x'_2 &= x_2 + \frac{K_1}{2\pi} \sin(2\pi x_1) - \frac{B}{2\pi} \{ \sin[2\pi(x_5 - x_1)] + \sin[2\pi(x_3 - x_1)] \} \\
 x'_3 &= x_3 + x'_4 \\
 x'_4 &= x_4 + \frac{K_2}{2\pi} \sin(2\pi x_3) - \frac{B}{2\pi} \{ \sin[2\pi(x_1 - x_3)] + \sin[2\pi(x_5 - x_3)] \} \pmod{1} \\
 x'_5 &= x_5 + x'_6 \\
 x'_6 &= x_6 + \frac{K_3}{2\pi} \sin(2\pi x_5) - \frac{B}{2\pi} \{ \sin[2\pi(x_3 - x_5)] + \sin[2\pi(x_1 - x_5)] \}
 \end{aligned}$$

3D torus

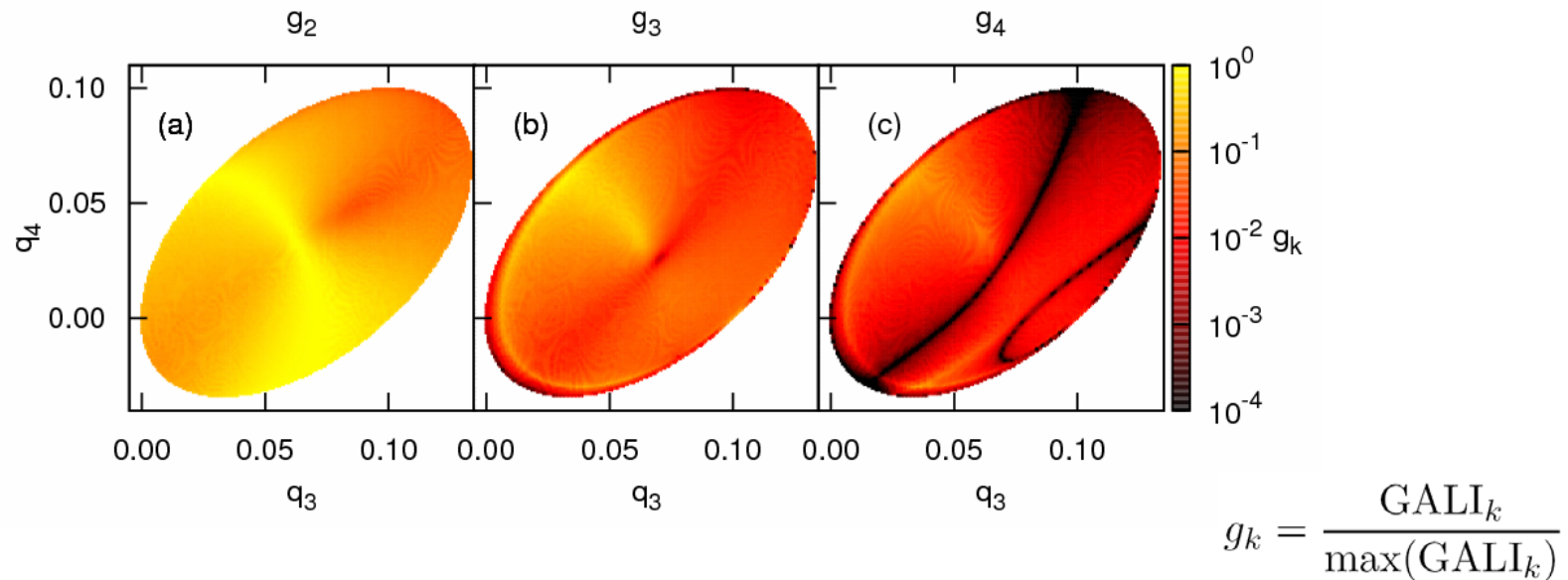


2D torus



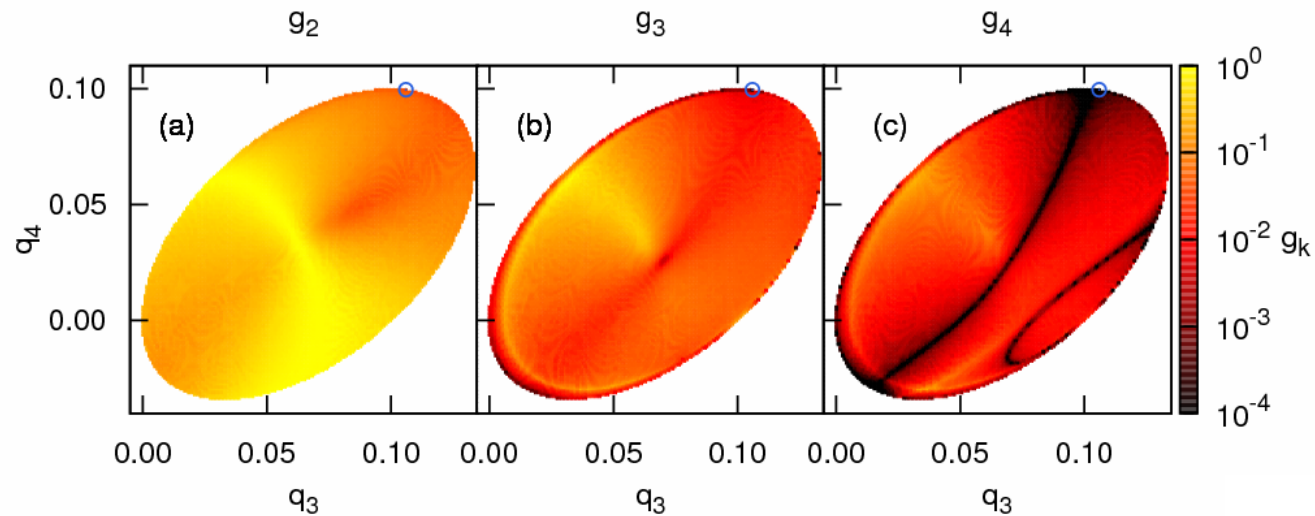
Locating low-dimensional tori

Orbits with $q_1=q_2=0.1$, $p_1=p_2=p_3=0$, $H=0.010075$ for the **N=4** FPU system (Gerlach, Eggl, Ch.S., 2011, nlin.CD/1104.3127).

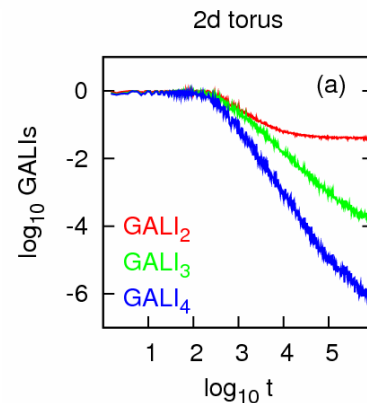


Locating low-dimensional tori

Orbits with $q_1=q_2=0.1$, $p_1=p_2=p_3=0$, $H=0.010075$ for the **N=4** FPU system (Gerlach, Eggl, Ch.S., 2011, nlin.CD/1104.3127).

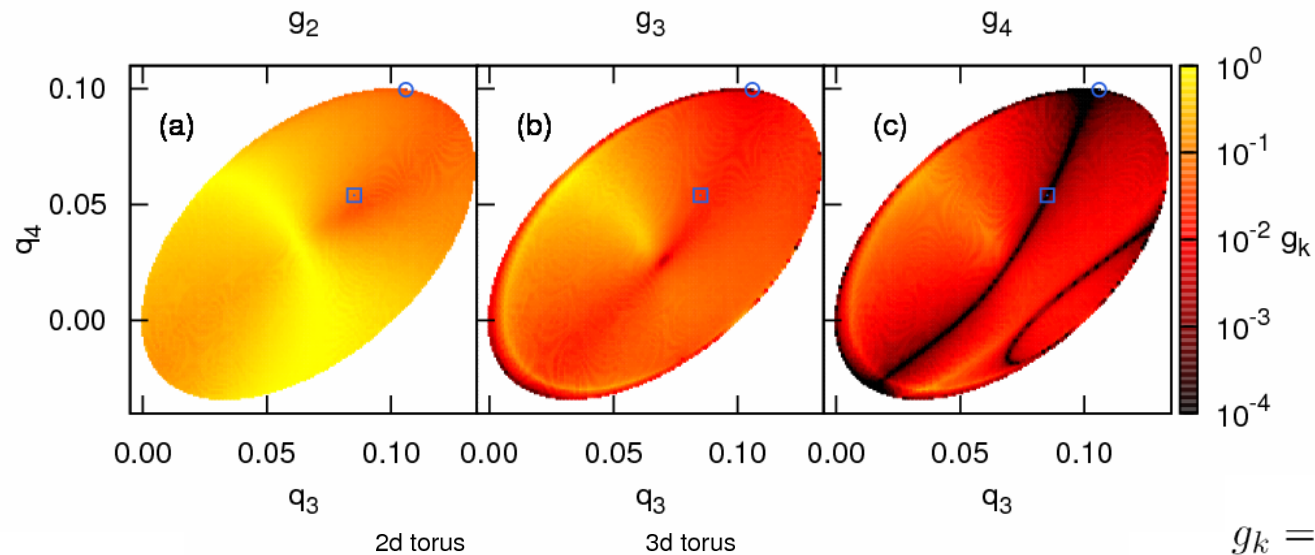


$$g_k = \frac{\text{GALI}_k}{\max(\text{GALI}_k)}$$

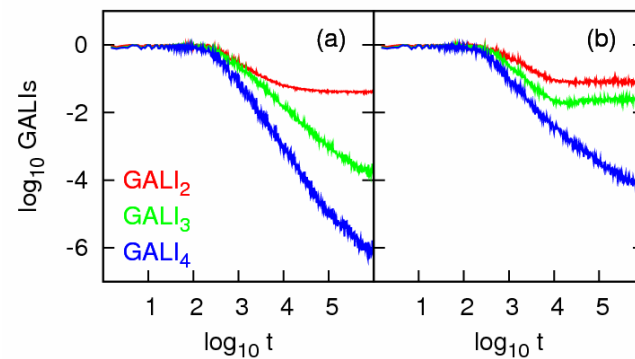


Locating low-dimensional tori

Orbits with $q_1=q_2=0.1$, $p_1=p_2=p_3=0$, $H=0.010075$ for the **N=4** FPU system (Gerlach, Eggl, Ch.S., 2011, nlin.CD/1104.3127).

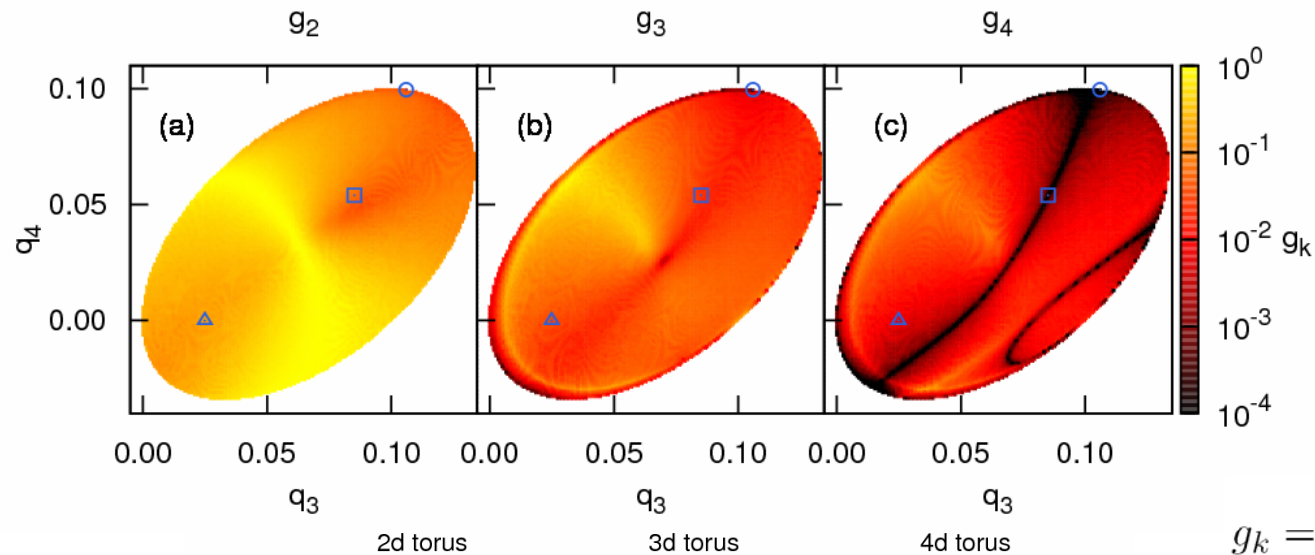


$$g_k = \frac{\text{GALI}_k}{\max(\text{GALI}_k)}$$

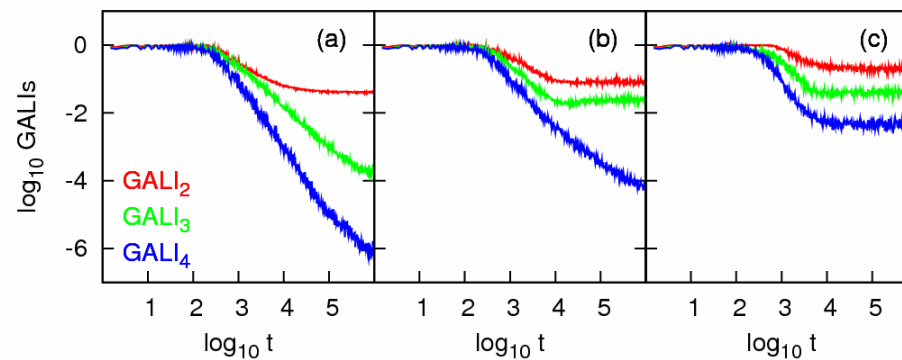


Locating low-dimensional tori

Orbits with $q_1=q_2=0.1$, $p_1=p_2=p_3=0$, $H=0.010075$ for the **N=4** FPU system (Gerlach, Eggl, Ch.S., 2011, nlin.CD/1104.3127).



$$g_k = \frac{\text{GALI}_k}{\max(\text{GALI}_k)}$$



Conclusions

- Generalizing the SALI method we define the Generalized Alignment Index of order k ($GALI_k$) as the volume of the generalized parallelepiped, whose edges are k unit deviation vectors. $GALI_k$ is computed as the product of the singular values of a matrix (SVD algorithm).
- Behaviour of $GALI_k$:
 - ✓ Chaotic motion: it tends exponentially to zero with exponents that involve the values of several Lyapunov exponents.
 - ✓ Regular motion: it fluctuates around non-zero values for $2 \leq k \leq s$ and goes to zero for $s < k \leq 2N$ following power-laws, with s being the dimensionality of the torus.

Conclusions

- $GALI_k$ indices :
 - ✓ can distinguish rapidly and with certainty between regular and chaotic motion
 - ✓ can be used to characterize individual orbits as well as "chart" chaotic and regular domains in phase space.
 - ✓ are perfectly suited for studying the global dynamics of multidimensional systems
 - ✓ can identify regular motion on low-dimensional tori
- SALI/GALI methods have been successfully applied to a variety of conservative dynamical systems of
 - ✓ Celestial Mechanics (e.g. Széll et al., 2004, MNRAS - Soulis et al., 2008, Cel. Mech. Dyn. Astr. - Libert et al., 2011, MNRAS, in press)
 - ✓ Galactic Dynamics (e.g. Capuzzo-Dolcetta et al., 2007, Astroph. J. - Carpintero, 2008, MNRAS - Manos & Athanassoula, 2011, MNRAS, in press)
 - ✓ Nuclear Physics (e.g. Macek et al., 2007, Phys. Rev. C - Stránský et al., 2007, Phys. Atom. Nucl. - Stránský et al., 2009, Phys. Rev. E)
 - ✓ Statistical Physics (e.g. Manos & Ruffo, 2010, nlin.CD/1006.5341)

Outlook

- Behavior of GALI_k indices :
 - ✓ for time dependent Hamiltonians
 - ✓ for systems with additional integrals of motion
 - ✓ for **dissipative systems**
 - ✓ for **time series**
 - ✓ near the boundary of stability islands, where the phenomenon of **stickiness** is prominent
- Characteristics of GALI_k indices :
 - ✓ estimation of the limiting GALI_k value for regular orbits of multidimensional systems
- Applications
 - ✓ **models studied at UCT**
 - ✓ identification of the selftrapped and spreading parts of wave packets in **disordered nonlinear lattices**
 - ✓ performance optimization of **real accelerators**
- Other chaos detection techniques
 - ✓ Computation of the spectrum of LCEs using the **compound matrix theory**
 - ✓ **Review paper:** Comparative study of the various existing methods

Main references

- **SALI**
 - ✓ Ch.S. (2001) J. Phys. A, 34, 10029
 - ✓ Ch.S., Antonopoulos Ch., Bountis T. C. & Vrahatis M. N. (2003) Prog. Theor. Phys. Supp., 150, 439
 - ✓ Ch.S., Antonopoulos Ch., Bountis T. C. & Vrahatis M. N. (2004) J. Phys. A, 37, 6269
- **GALI**
 - ✓ Ch.S., Bountis T. C. & Antonopoulos Ch. (2007) Physica D, 231, 30-54
 - ✓ Ch.S., Bountis T. C. & Antonopoulos Ch. (2008) Eur. Phys. J. Sp. Top., 165, 5-14
 - ✓ Manos T., Ch.S. & Antonopoulos Ch. (2011) arXiv:nlin.CD/1103.0700
- **Lyapunov exponents**
 - ✓ Ch.S. (2010) Lect. Notes Phys., 790, 63-135